OKLAHOMA TRANSPORTATION CENTER

ECONOMIC ENHANCEMENT THROUGH INFRASTRUCTURE STEWARDSHIP

DRYING SHRINKAGE PROBLEMS IN HIGH-PLASTIC CLAY SOILS IN OKLAHOMA

RIFAT BULUT, PH.D., P.E.
MUSHARRAF ZAMAN, PH.D., P.E.
OMAR AMER
SRUTHI MANTRI
LIZHOU CHEN
YI TIAN
ALI TAGHICHIAN

OTCREOS11.1-09-F

Oklahoma Transportation Center
2601 Liberty Parkway, Suite 110
Midwest City, Oklahoma 73110

Phone: 405.732.6580
Fax: 405.732.6586
www.oktc.org

DISCLAIMER

The contents of this report reflect the views of the authors, who are responsible for the facts and accuracy of the information presented herein. This document is disseminated under the sponsorship of the Department of Transportation University Transportation Centers Program, in the interest of information exchange. The U.S. Government assumes no liability for the contents or use thereof.

TECHNICAL REPORT DOCUMENTATION PAGE

1. REPORT NO.	2. GOVERNMENT ACCESSION NO.	3. RECIPIENTS CATALOG NO.
OTCREOS11.1-09-F		

4. TITLE AND SUBTITLE	5. REPORT DATE
Drying Shrinkage Problems in High-Plastic Clay Soils in Oklahoma	August 2013
	6. PERFORMING ORGANIZATION CODE

7. AUTHOR(S)	8. PERFORMING ORGANIZATION REPORT
Rifat Bulut, Musharraf Zaman, Omar Amer, Sruthi Mantri, Lizhou Chen, Yi Tian, and Ali Taghichian	

9. PERFORMING ORGANIZATION NAME AND ADDRESS	10. WORK UNIT NO.
Oklahoma State University School of Civil and Environmental Engineering 207 Engineering South, Stillwater, OK 74078	11. CONTRACT OR GRANT NO. DTRT06-G-0016

12. SPONSORING AGENCY NAME AND ADDRESS	13. TYPE OF REPORT AND PERIOD COVERED
Oklahoma Transportation Center (Fiscal) 201 ATRC, Stillwater, OK 74078 (Technical) 2601 Liberty Parkway, Suite 110, Midwest City, OK 73110	Final Feb. 2012 - April 2013 14. SPONSORING AGENCY CODE

15. SUPPLEMENTARY NOTES
University Transportation Center and The University of Oklahoma

16. ABSTRACT

Longitudinal cracking in pavements due to drying shrinkage of high-plastic subgrade soils has been a major problem in Oklahoma. Annual maintenance to seal and repair these distress problems costs significant amount of money to the state. The longitudinal cracks occur usually within the so-called edge moisture variation distance, where the climate plays a significant role in terms of changes in moisture content. The current study investigated the longitudinal drying shrinkage problems in pavement subgrade soils at three sites in Oklahoma. Two of the sites located in Norman and Oklahoma City are bike trails and the third site is along the Interstate Highway I-35 in Ardmore. The soil specimens collected from these sites were tested for the basic index properties as well as suction and unsaturated diffusivity measurements. Various ranges of the test results have been implemented in a suction profile and tensile stress prediction models for evaluating the typical suction changes and the corresponding tensile stresses in subgrade soils

17. KEY WORDS	18. DISTRIBUTION STATEMENT
Drying, shrinkage, pavement, suction	No restrictions. This publication is available at www.oktc.org and from the NTIS.

19. SECURITY CLASSIF. (OF THIS REPORT)	20. SECURITY CLASSIF. (OF THIS PAGE)	21. NO. OF PAGES	22. PRICE
		97 + covers	

SI (METRIC) CONVERSION FACTORS

Approximate Conversions to SI Units

Symbol	When you know	Multiply by	To Find	Symbol
	LENGTH			
in	inches	25.40	millimeters	mm
ft	feet	0.3048	meters	m
yd	yards	0.9144	meters	m
mi	miles	1.609	kilometers	km
	AREA			
in^2	square inches	645.2	square millimeters	mm
ft^2	square feet	0.0929	square meters	m^2
yd^2	square yards	0.8361	square meters	m^2
ac	acres	0.4047	hectares	ha
mi^2	square miles	2.590	square kilometers	km^2
	VOLUME			
fl oz	fluid ounces	29.57	milliliters	mL
gal	gallons	3.785	liters	L
ft^3	cubic feet	0.0283	cubic meters	m^3
yd^3	cubic yards	0.7645	cubic meters	m^3
	MASS			
oz	ounces	28.35	grams	g
lb	pounds	0.4536	kilograms	kg
T	short tons (2000 lb)	0.907	megagrams	Mg
	TEMPERATURE (exact)			
°F	degrees Fahrenheit	(°F-32)/1.8	degrees Celsius	°C
	FORCE and PRESSURE or STRESS			
lbf	poundforce	4.448	Newtons	N
lbf/in^2	poundforce per square inch	6.895	kilopascals	kPa

Approximate Conversions from SI Units

Symbol	When you know	Multiply by	To Find	Symbol
	LENGTH			
mm	millimeters	0.0394	inches	in
m	meters	3.281	feet	ft
m	meters	1.094	yards	yd
km	kilometers	0.6214	miles	mi
	AREA			
mm^2	square millimeters	0.00155	square inches	in^2
m^2	square meters	10.764	square feet	ft^2
m^2	square meters	1.196	square yards	yd^2
ha	hectares	2.471	acres	ac
km^2	square kilometers	0.3861	square miles	mi^2
	VOLUME			
mL	milliliters	0.0338	fluid ounces	fl oz
L	liters	0.2642	gallons	gal
m^3	cubic meters	35.315	cubic feet	ft^3
m^3	cubic meters	1.308	cubic yards	yd^3
	MASS			
g	grams	0.0353	ounces	oz
kg	kilograms	2.205	pounds	lb
Mg	megagrams	1.1023	short tons (2000 lb)	T
	TEMPERATURE (exact)			
°C	degrees Celsius	9/5+32	degrees Fahrenheit	°F
	FORCE and PRESSURE or STRESS			
N	Newtons	0.2248	poundforce	lbf
kPa	kilopascals	0.1450	poundforce per square inch	lbf/in^2

ACKNOWLEDGEMENTS

The authors would like to express their thanks to the Oklahoma Department of Transportation for providing soil specimens for this project.

DRYING SHRINKAGE PROBLEMS IN HIGH-PLASTIC CLAY SOILS IN OKLAHOMA

Final Report

August 2013

By Rifat Bulut, Ph.D., Omar Amer, Sruthi Mantri, Lizhou Chen, and Yi Tian

Oklahoma State University

and

Musharraf Zaman, Ph.D., P.E and Ali Taghichian

The University of Oklahoma

Sponsored by the

Oklahoma Transportation Center

Oklahoma State University

207 Engineering South

Stillwater, OK 74078

and

The University of Oklahoma

202 W. Boyd Street

Norman, OK 73019

TABLE OF CONTENTS

LIST OF FIGURES

LIST OF TABLES

EXECUTIVE SUMMARY

Longitudinal cracking in pavements due to drying shrinkage of high-plastic subgrade soils has been a major problem in Oklahoma. Annual maintenance to seal and repair these distress problems costs significant amount of money to the state. The longitudinal cracks occur usually within the so-called edge moisture variation distance, where the climate plays a significant role in terms of changes in moisture content. The current study investigated the longitudinal drying shrinkage problems in pavement subgrade soils at three sites in Oklahoma. Two of the sites located in Norman and Oklahoma City are bike trails and the third site is along the Interstate Highway I-35 in Ardmore. The soil specimens collected from these sites were tested for the basic index properties as well as suction and unsaturated diffusivity measurements. Various ranges of the test results have been implemented in suction profile and tensile stress prediction models for evaluating the typical suction changes and the corresponding tensile stresses in subgrade soils.

In recent years, a significant effort has been directed to better analyze the ground and climate interactions as applicable to a range of transportation structures. Drying shrinkage cracking in the pavement structure has been a major problem in Oklahoma. In many cases, this type of cracking initiates in the drying subgrade soil and reflects from the highly plastic subgrade through the pavement structure. The relatively impermeable pavement surface has a significant impact on the formation of the non-uniform moisture profiles. The mechanism of crack development, therefore, is rooted in the moisture (suction) variation in the shrinking high PI subgrade soil. The gradients of moisture variation, together with the soil volume change characteristics, determine the tensile stress distribution and shrinkage crack initiation. The study indicates that the drying shrinkage problem should be investigated based on the unsaturated soil mechanics principles and the climate surface and subsurface boundary conditions. The study has helped in improving our understanding of the mechanism of drying shrinkage problems in high-plastic soils using the unsaturated soil mechanics principles. The report provides a rational approach in predicting the moisture (suction) change regime underneath the pavement and corresponding tensile stresses in subgrade soils.

1. INTRODUCTION

The problems associated with shrinking and swelling soils are worldwide. In the United States, approximately 20 percent of the area is underlain by moderately to highly expansive soil. The annual cost of damage in the United States from shrinking and swelling soils is estimated at over $15 billion, and close to half this damage is attributed to highways and streets. Longitudinal cracking in pavements due to drying shrinkage of high-plastic subgrade clays has been a major problem in Oklahoma. Annual maintenance to seal and repair these distress problems can cost millions of dollars statewide. It has been well established in the literature that the mechanisms of shrinkage cracks due to high PI clay soils are governed by the principles of unsaturated soil mechanics, the suction stress being the major part of the cracking mechanism. These longitudinal cracks occur usually within the so-called edge moisture variation distance, where the climate plays a significant role in terms of changes in water content (or suction). Thus, the drying shrinkage problem should be investigated based on the unsaturated soil mechanics principles and the climate surface and subsurface boundary conditions.

The current study investigates the subgrade soils at three sites in Oklahoma that have experienced drying shrinkage problems. Shelby tube soil specimens were obtained from the sites in Norman, Lake Hefner, and Ardmore in Oklahoma for laboratory testing. The soil specimens were tested for the basic index properties as well as suction and unsaturated diffusivity measurements. Test results have been implemented in a suction prediction model for evaluating typical suction profiles in subgrade soils. An existing, water-content based analytical model was modified for unsaturated soils for prediction of tensile stresses in subgrade soils. The analytical model is currently being evaluated in the accompanying on-going research project using a commercially available software package for the prediction of suction profiles and tensile

stresses in subgrade soils. The results will be included in the comprehensive final report to ODOT.

1.1 Problem Statement

Longitudinal cracking in pavements due to drying shrinkage of high PI subgrade clays has been a major problem in Oklahoma. These cracks occur close to the shoulder of the pavement where the climate plays a significant role in terms of changes in water content (suction). Annual maintenance to repair these distress problems can cost millions of dollars to Oklahoma. The study to understand these problems includes laboratory soil testing for unsaturated soil properties, basic soil index parameters, and modeling.

1.2 Objectives

This study focuses on improving our understanding of the mechanism of drying shrinkage problems in high-plastic soils using the unsaturated soil mechanics principles. The project attempts to provide a rational approach in predicting the moisture (suction) change regime underneath the pavement and corresponding tensile stresses in subgrade soils. The study attempts to provide practical analyses methods for design of pavements on potentially shrinking clay soils. The study includes laboratory soil testing from the three problem sites in Oklahoma, and modeling. The specific objectives of this study are:

1) to address the failure mechanisms leading to the occurrence of the shrinkage cracks from the subgrade to the pavement surface, and
2) to provide analytical and theoretical support to the analysis of the problem.

1.3 Organization of Report

This report consists of seven major chapters. Chapter one provides general information, problem statement, and objectives of the study. Chapter two provides background information on the drying shrinkage problem in unsaturated soils. Chapter three covers the sites and soil descriptions for the Norman, Lake Hefner, and Ardmore pavement sites. Chapter four explains the laboratory testing program conducted in this study and test results. Chapter five describes the analytical models for the suction and tensile stress profiles in unsaturated soils. Chapter six makes some conclusions about the study. The report also provides the cited references and appendices including all the test results.

THIS PAGE IS INTENTIONALLY LEFT BLANK

2. BACKGROUND

High PI shrinking clay soils are encountered in many parts of Oklahoma. These subgrade soils support transportation infrastructure, which include pavements, runways, parking lots, bike and walking trails at the recreational areas, etc. Damages to civil infrastructures due to shrinking soils have been increasing each year as a result of large volumetric strains experienced by these soils from moisture content fluctuations. Longitudinal pavement cracking on the local road network in Oklahoma is one of the most prevalent pavement distresses caused by volumetric changes of shrinking high PI subgrade soils (Nevels 2006). These cracks occur close to the shoulder of the pavement and represent a significant problem for Oklahoma Department of Transportation (ODOT) as well as other state agencies. Annual maintenance to seal and repair these distress problems can cost millions of dollars statewide. In the United States, volumetric changes due to shrinking and swelling soils cause extensive damage, which costs about $7 to $15 billion annually (Nuhfer et al. 1993; Wray and Meyer 2004).

Desiccation of clay soils causes shrinkage cracks which is a major problem in pavement engineering as well as in some other disciplines (Jayatilaka et al. 1993; Puppala et al. 2009). Shrinkage cracks have the potential to cause severe damage to the serviceability of the transportation infrastructure. In recent years, a significant effort is directed to better analyze ground and climate interactions as applicable to a range of transportation structures. It has been well established in the literature that the mechanism of shrinkage cracks due to high PI clay soils are governed by the principles of unsaturated soil mechanics, the suction stress being the major part of the cracking mechanism (Luo and Prozzi 2008; Puppala et al. 2009).

In many cases, this type of cracking initiates in the drying subgrade soil and reflects from the highly plastic subgrade through the pavement structure. These longitudinal cracks occur usually

within the so-called edge moisture variation distance (e_m), where the climate plays a significant role in terms of changes in water content (suction). Climatic effects have long been recognized as being influential in the construction and performance of pavements (Lytton et al. 2005). Consequently, the drying shrinkage problem should be investigated based on the unsaturated soil mechanics principles and the climatic surface and subsurface boundary conditions. The mechanism of crack development is rooted in the moisture variation in shrinking high PI subgrade soil. The impermeable pavement surface layer has a significant impact on water migration out of the shrinking subgrade beneath the pavement, which results in the non-uniform moisture change in the subgrade (Luo and Prozzi 2009). The gradients of moisture variation, together with the soil volume change characteristics, determine the tensile stress distribution and shrinkage crack initiation.

If the initial condition is considered after the subgrade construction when the subgrade soil is intact without any cracks, the initial strains are zero in all three directions (Luo and Prozzi 2009). During the desiccation process of the soil in the pavement subgrade, the lateral strains (the strains in horizontal directions) remain zero before crack initiation because of lateral constraint (Luo 2007). The field data collected by Konrad and Ayad (1997) confirmed that drying soils experience a restrained desiccation so that the lateral strains were maintained zero until a crack initiated in the soil. As a result, the incremental horizontal strains in both transverse and longitudinal directions remain zero before cracking. However, soils are considered to have a certain amount of tensile strength, and this tensile strength has been used in the crack initiation criterion that predicts the onset of large tensile cracks by comparing the tensile strength with the net normal horizontal stress (Ayad et al. 1997).

In order to study the development of desiccation cracks in the subgrade soil during the reduction in water content and increase of matric suction, it is desirable to estimate the shrinkage stresses generated between two steady state matric suction profiles. Lytton et al. (2005) used a volumetric strain based model for the computations of displacements between two suction profiles (i.e., dry suction profile and wet suction profile). Sumarac (2004) presented a simpler approach for the prediction of the tensile stresses based on the elastic theory in response to suction changes.

Consequently, the shrinkage stress produced by the matric suction change can be estimated using the stress-strain constitutive relationships of the subgrade soil. Based on the stress distribution, the development of shrinkage cracks can be analyzed. A theoretical, but practical, approach is needed to identify and analyze the mechanisms of the longitudinal crack development and to minimize this type of crack by means of economical and practical means. An understanding of these mechanisms is necessary to design economical remedial maintenance programs and to alter future designs, construction methods, and material specifications to reduce or eliminate this type of pavement stress. To understand the mechanisms of pavement cracking, it is necessary to understand the major variables which initiate the cracks. In the mechanisms mentioned here, it is evident that climatic effects have a major influence on the behavior of pavements.

2.1 Moisture Diffusion in Unsaturated Soils – Matric Suction Profiles

The matric suction profile in the soil can be predicted theoretically by solving the moisture diffusion equations that governs the matric suction distribution in the soil. Mitchell (1979) proposed solutions to the general moisture diffusion equation for several different boundary conditions to simulate the effects of climate on matric suction at the ground surface, and with depth at any time. The magnitude and rate of transient moisture flow in an unsaturated soil in

response to suction changes is controlled by the unsaturated moisture diffusion coefficient, which is a fundamental soil parameter in Mitchell's model (Mabirizi and Bulut 2010).

The equilibrium matric suction is usually estimated for different climatic regions based on the Thornthwaite Moisture Index (TMI). The TMI has shown promise in relating climate to pavement performance (Jayatilaka et al. 1993). The TMI is a climatic parameter introduced by Thornthwaite (1948) to characterize the moisture balance in a specific location taking into account climatic variables as rainfall, potential evapotranspiration and the depth of available moisture stored in the root zone of the vegetation. The original Thornthwaite (1948) approach for computing the TMI maps were later simplified further by Thornthwaite and Mather (1955) and Witzack et al. (2006). As a result of the revision, the modified TMI is only related to the precipitation and potential evapotranspiration at monthly intervals in evaluating the annual soil moisture balance. The Witzack et al. (2006) study was conducted as part of the Enhanced Integrated Climatic Model (EICM) in the Mechanistic Empirical Pavement Design Guide (MEPDG), and correlations were established between TMI and equilibrium suction at depth in the pavement profile. The equilibrium suction can also be measured in the field, or estimated from Mitchell's model.

2.2 Unsaturated Soil Volumetric Strains

In unsaturated soils, two stress state variables (i.e., matric suction and mean mechanical stress) play a significant role in determining shear strength and volume change characteristics of soils (Fredlund and Morgenstern 1977). Luo and Prozzi (2009) indicated that the Lytton's model (i.e., Lytton et al. 2005), incorporating the two stress state variables for volumetric strains and Mitchell's diffusion equations for suction profiles, provides a reasonable and relatively simple relation for studying the longitudinal shrinkage cracks in pavement subgrade soils. However, in

their study, Luo and Prozzi (2009) did not consider the effects of the mean mechanical stress, only suction stresses were considered. This was a reasonable assumption because in pavements the effects of mean mechanical stresses on the development of shrinkage cracks are probably small and negligible, as compared to the effects of suction stresses.

This stress-strain analysis uses unsaturated soil mechanics principles to analyze the suction stress distribution in the pavement structure over shrinking subgrade soils. The matric suction stress distribution before crack initiation is critical in order to investigate the potential location and propagation of the shrinkage crack. As the moisture content decreases in the subgrade soil, the matric suction increases, which results in volumetric changes of the soil (Sabnis et al. 2010). If the matric suction change is uniform and the soil is not constrained, normal strains will occur in each direction unaccompanied by normal stresses (Kodikara et al. 2002; Luo and Prozzi 2009). However, because the pavement is an impermeable cover, the matric suction change is not uniform in the subgrade soil. In addition, the lateral confinement does not allow the soil to have free expansion or shrinkage. Therefore, tensile stresses will occur as the matric suction increases. As the tensile stress reaches the tensile strength of the soil, a shrinkage crack will initiate in the subgrade.

2.3 Tensile Stresses and Formation of Shrinkage Cracks

It is believed that there are at least two opinions in the literature about the mechanisms involved in the formation of the shrinkage cracks and their propagation to the pavement surface (Crockford and Little 1987; Lytton et al. 2005; Luo and Prozzi 2009; Sumarac 2004). In one of the mechanisms, the soil will shrink within the edge-moisture variation distance in the vertical direction, and the asphalt concrete layer will deflect with the shrinking soil in a cantilever like action, and cause very high tensile stresses resulting from the bending action on the surface of

the asphalt layer. Luo and Prozzi (2009) used the Lytton et al. (2005) approach in analyzing the shrinkage strains and the corresponding stresses using an elastic theory as mentioned in the previous section.

In the other mechanism, the shrinkage crack will initiate in the soil if the tensile shrinkage stress exceeds the tensile strength of the soil. After the crack initiation, the propagation of the crack depends on a number of factors, including loading condition, the crack length, and boundary conditions (Crockford and Little 1987). The progression of the initial crack is critical to the development of the longitudinal crack found on the pavement surface (Ayad et al. 1997). Sumarac (2004) investigated this problem utilizing a simpler but practical approach using elastic theory.

Since these high PI soils will shrink in three-dimensions (but not necessarily in equal amounts in each direction) it is very reasonable that both of the failure mechanisms occur at the same time. However, one of those failure mechanisms could dominate the occurrence of the surface longitudinal cracks depending on several factors including the bonding strength between the high PI subgrade layer and the layer above it (as well as the fracture toughness of the material above the shrinking soil), the magnitudes of suction stress that will cause shrinkage cracks and horizontal strains, and the magnitude of volume change in the vertical direction (Lytton et al. 2005; Luo and Prozzi 2008; Puppala et al. 2009). While determination of the initial conditions for formation of the cracks is critical, the analysis of crack propagation in the pavement was also investigated by researchers (Luo and Prozzi 2009; Ayad et al. 1997). Luo and Prozzi (2009) studied the crack propagation problem from the strain energy release point of view using the finite element method. At energy equilibrium, the strain energy release rate is equal to the surface energy of the generated two crack surfaces. The strain energy release rate (i.e., the

surface free energy of the crack surface) is a function of the stress intensity factor (the fracture toughness of the material), which is a constant material property and can be measured in the laboratory. The direct experimental determination of the fracture toughness of a clayey soil is, however, very difficult. Instead, the fracture toughness can be inferred from other material constants, which in turn can be determined from laboratory tests or inferred from known relationships (Ayad et al. 1997). The fracture toughness of different soils and other pavement materials have been measured in the laboratory (Harrison et al. 1994; Crockford and Little 1987). When the stress intensity factor is larger than the fracture toughness of the material, the crack is unstable and will propagate to release energy until the equilibrium is reached. When the stress intensity factor is smaller than the fracture toughness, the crack remains stable. The fracture toughness of the soil should also depend on its current matric suction level. The initiation and propagation of the shrinkage cracks can be evaluated using a finite element analysis.

Long (2006) performed numerical simulations to study the field moisture diffusivity using a conceptual model of moisture diffusion in a cracked soil mass. A rough correlation between field and laboratory measurements of moisture diffusion coefficients has been presented for different crack depth patterns. Shrinkage cracks have significant effects on the soil's diffusivity parameter, and can be modeled in the laboratory under controlled conditions. Recently, Mabirizi and Bulut (2010) conducted drying and wetting tests on different high plasticity clay soils, and have found significant differences in diffusivity between the cracked and intact soils.

This complex stress-strain field in the pavement subgrade layer, resulting from moisture content (suction) changes, requires a comprehensive approach for the analysis of the shrinkage cracking problems in high-plastic subgrade soils. A detailed laboratory testing program is needed to determine the basic index properties and unsaturated parameters of the high PI shrinking soils.

Although there are several models available in the literature, the numbers and characteristics of the parameters of the models are complex, and their determination is time consuming and expensive. Simple and practical approaches are needed to understand and analyze the moisture diffusion process and development of tensile stresses in the soil. A shrinkage crack will initiate in the soil if the tensile shrinkage stress exceeds the tensile strength of the soil.

3. SITE AND SOIL DESCRIPTION

Soil specimens from three sites in Oklahoma that are experiencing drying shrinkage problems were obtained for laboratory soil testing. Oklahoma Department of Transportation (ODOT) conducted the drilling process and sampled Shelby tube soil specimens for this project. These sites are located in Oklahoma City near Lake Hefner (named as Lake Hefner site), in Norman on Robinson Street (named as Norman site), and along Interstate Highway I-35 in Ardmore (named as Ardmore site) in Oklahoma. Both Lake Hefner and Norman sites are bike trails about 12 feet wide constructed using a thin layer of base material with a thin layer of asphalt concrete on top. The bike trail at the Lake Hefner site is located east of Lakeshore Drive in Lakeshore Park, which is in southwest side of Lake Hefner. The bike trail at the Norman site is located north of West Robinson Street at the intersection of West Robinson Street and Woods Avenue. The Ardmore site along I-35 is located between 12th Avenue and Veterans Boulevard. According to ODOT, the sites have been experiencing longitudional cracks due to drying shrinkage of high plastic subgrade soils for number of years.

The research team visited both Norman and Lake Hefner sites for the visual inspection of the sites and the cracks. The shrinkage cracks in the asphalt material at the Norman site were covered by asphalt emulsion. Therefore, the size of the cracks were not that visible. However, from the nature of the surface treatment and close visual inspection, the size and length of the cracks seemed significant. Figure 3.1 depicts a picture of the sealed cracks at the Norman site. Longitudinal cracks due to drying shirnkage of high plastic subgrade soils were clearly visible at the Lake Hefner site. Figure 3.2 shows the longitudinal cracks along the bike trail at the Lake Hefner site. The cracks were mostly along the shoulder of the pavement. The cracks were from about a few milimeters to about 30 milimeters wide.

Figure 3.1 Longitudinal Drying Shrinkage Problem at Norman Site.

Figure 3.2 Longitudinal Drying Shrinkage Problem at Lake Hefner Site.

3.1 Soil Sampling

ODOT collected soil specimens using Shelby tubes at four boring holes at the Norman site. Push tubes were driven to the depths of 3.8, 17.1, 17.7, and 17.8 feet for obtaining undisturbed Shelby tube specimens. These specimens were collected from the ODOT's main office in Oklahoma City and brought to Oklahoma State University for laboratory testing. Immediately after that a comprehensive visual inspection and description of the specimens was conducted. The results of the visual inspection are provided in Appendix A.

ODOT made three boring holes at the Lake Hefner site to depths of 9.9, 8.7, and 8.5 feet for obtaining undisturbed Shelby tube specimens. The push tube specimens were collected from the ODOT's main office in Oklahoma City and carried to Oklahoma State University for visual inspection and laboratory testing. The results of the visual inspection and soil descriptions are given in Appendix B.

Seven boring holes were made by ODOT at the Ardmore site along the Interstate Highway I-35 for collecting Shelby tube specimens. The push tubes were driven to the depths of 3.57, 3.45, 6.0, 8.0, 8.0, 8.0, and 8.0 feet for sampling. These specimens were delivered to OSU labs by ODOT for laboratory testing in this study. Immediately after the arrival of the specimens a comprehensive visual inspection and description of the samples were performed. The details of the inspection are provided in Appendix C.

3.2 Conditions of Soil Specimens and Their Descriptions

The soil specimens from all the three sites were significantly disturbed and were in very dry conditions with suction values close to 5 pF. As it is known the wilting point of vegetation is around 4.5 pF. This indicates that the soils were extremely. Due to the very severe drought

season in 2012, the specimens were very dry, with various sizes of shrinkage cracks and root fibers. The poor conditions of the specimens have created significant amount of difficulty in setting up the specimens for laboratory testing. One major problem was with the drying diffusion coefficient measurement test setups using the thermocouple psychrometers. Thermocouple psychrometers function properly when the suction in the soil is in between about 3.7 pF and 4.7 pF. The extremely dry specimens, therefore, we exposed to a wetting process before they can be setup for the drying diffusion coefficient measurements. Since the conditions of the specimens were not that good (i.e., significant amount disturbance, cracks, and root fibers), some of the test specimens simply failed during the wetting-drying process. Another problem with the soil samples was the short length of the specimens. The diffusion test requires soil specimens of at least 25-30 cm in length, so that the initial suction condition of the soil can be determined in the proximity of the diffusion test specimen.

In an ideal condition, all the tests need to be performed on the same soil specimens for the proper interpretation of the test results. Due to the significant amount of sample disturbance, this was not possible. Furthermore, in order to reduce the number of tests and determine the soil parameters on the different soil types, the research team grouped the specimens from each site into Soil Types based on their visual inspection (i.e., mostly color and to some extent the texture). The different soil types identified for the Norman, Lake Hefner, and Ardmore sites are given in Appendix A, Appendix B, and Appendix C, respectively.

4. LABORATORY SOIL TESTS

This chapter discusses the laboratory soil tests conducted at Oklahoma State University. The tests are conducted on the soil specimens collected from the three sites located in the state of Oklahoma named Norman, Lake Hefner, and Ardmore. Shelby tube specimens were sampled by the Oklahoma Department of Transportation (ODOT) and delivered to OSU for testing. The different tests conducted are the Atterberg limits, water content, hydrometer analysis, sieve analysis, compaction, suction measurements using the filter paper, chilled-mirror dew-point psychrometer, and thermocouple psychrometers, and drying diffusion coefficient measurements. In total, 28 drying diffusion coefficient tests were conducted. Water content and total suction measurements were determined for at least every soil specimen set for the drying diffusion coefficient test. All the received soil specimens were stored in a temperature-controlled room in sealed condition in ice-chests. The laboratory determination of water content was conducted using the ASTM D2216 for all the specimens selected for the drying diffusion test. Other tests are performed on every type of soil identified throughout a visual inspection and identification process described in the previous chapter and appendix.

4.1 Atterberg Limits

Liquid limit and plastic limit tests were conducted in accordance with the ASTM D4318. The liquid and plastic limits correspond to different levels of consistencies in fine-grained soils. The values may vary according to the clay mineral type and percentage in the whole soil mixture. For the liquid and plastic limit tests, the soil sample was oven dried at 105 ± 5^{o}C. The sample was further broken into smaller pieces by using a hand rammer and then ground to finer particles using grinding machines. The ground sample was passed through the US sieve #40. The sample passing the sieve was collected and used for obtaining the Atterberg limits.

For conducting the liquid limit test, the samples were mixed with distilled water and placed in a ceramic cup for moisture conditioning for 24 hours. The ceramic cup was covered with plastic wrap to avoid moisture loss. After moisture conditioning, the liquid limit test was performed according to ASTM D4318. The plastic limit test was conducted on the same soil following the ASTM D4318 testing specifications.

4.2 Hydrometer Analysis

Hydrometer analysis is the test used to determine the grain size distribution of the soil particles passing the US sieve #200. The analysis is based on the Stoke's law which relates the terminal velocity of a falling sphere in a liquid to its diameter. A series of density measurements at known depth of suspension and at known times of settlement gives the percentages of particles finer than the diameters given by Stoke's law. The series of readings reflects the amount of different sizes of particles in the fine-grained soils. The ASTM D422-63 testing method was adopted for sample preparation and testing. A dispersing solution was prepared by mixing 40 grams of sodium hexametaphosphate in 1000 milliliters of distilled water. This solution is required for deflocculation of particles, as the clay particles have tendency to adhere to each other and form larger masses. Fifty grams of soil passing the US sieve #200 is required for the hydrometer analysis. The soil sample is mixed with 125 milliliters of dispersing solution. Finally, distilled water is added to a make a total of 1000 milliliters volume of suspended solution. The suspension is kept undisturbed, and readings are taken at 2, 5, 15, 30, 60, 240, 1440 minutes interval. The combined sieve and hydrometer analyses permitted estimates of the clay fraction of the soil.

4.3 Sieve Analysis

Fine-grained plastic clay particles tend to adhere together when dried, even when subjected to grinding. Therefore, dry sieve analysis of such clays is not usually recommended. To avoid this potential problem, a wet sieve analysis procedure was adopted. The wet sieving was followed according to ASTM D92-95. The sample was soaked in water for 2 hours in order to prevent the finer materials from adhering to the larger particles. The test specimen was then transferred to the sieve #200 for washing. With a small jet of water from a rubber hose, the sample was washed until the water passing through the sieve contains only traces of the specimen. Exercise of care during washing was performed to prevent loss by splashing. Then, the washed residue in the sieve was dried in the oven at 105±5^{o}C. The dried residue was transferred to coarser sieve for the analysis. The percentage of soil passing was calculated per ASTM D92-95.

4.4 Soil Compaction

Compaction tests were followed accoring to ASTM D1557-12. The soil sample was taken and oven dried for 24 hours. The sample was grounded and about 2000 grams of the sample was used for the compaction test. The soil sample was mixed with water and allowed to cure per ASTM D1557-12 guidelines. The mold and collar were assembled and secured to the base plate. The soil was compacted in three layers, each layer receiving 25 number of drops from 12 inches. After the compaction, the collar and base plate were removed from the mold. A knife was used to trim the soil at the top. The mass of the compacted specimen and mold was determined and recorded to the nearest gram. The compacted specimen was then removed from the mold using a hydraulic jack. The compaction curve was determined per ASTM D1557-12.

4.5 Soil Total Suction

Soil suction can simply be described as a measure of the ability of a soil to attract and hold water. It is the quantity of moisture energy that can be used to characterize the behavior of unsaturated soils. The filter paper method (as described in Bulut et al. 2001), chilled-mirror psychrometer (as described in Bulut et al. 2002), and thermocouple psychrometers (as described in Bulut and Leong 2008) have been used in determining the total suction characteristics of the soils. Thermocouple psychrometers were used with the CR7 datalogger and data acquisition system by the Wescor and Campbell Scientific. The filter paper method and chilled-mirror device were basically adopted for determining the initial total suction in the soil. On the other hand, thermocouple psychrometers were used for continuous monitoring and recording of total suctions for the unsaturated diffusion coefficient measurements.

4.6 Unsaturated Drying Diffusion Coefficient

The drying diffusion coefficient is measured in the laboratory based on the methodology proposed by Mitchell (1979). Based on the Mitchell's approach, a testing equipment and protocol developed at Oklahoma State University for measuring both the drying and wetting diffusion parameters as described in detail in Mabirizi and Bulut (2010). For the laboratory testing, the Shelby tube cylindrical soil specimens are sealed along the sides and one by plastic wrap, aluminum foil, and electrical tape. The other end of the specimen is left open to the laboratory atmosphere to permit the evaporation of the soil moisture in response to the suction gradient between the soil and laboratory atmosphere. Thermocouple psychrometers inserted in the sample measure the soil total suction at different time intervals. By measuring the suction and its corresponding time, the drying diffusion coefficient (α_{dry}) can be calculated. The other input parameters needed in the compuation of the diffusion parameter are the atmospheric suction,

initial total suction, evaporation coefficient, length of the specimen, and the location of the thermocouple psychrometer from the closed end.

4.7 Laboratory Test Results for Norman, Lake Hefner, and Ardmore Sites

As discussed in the previous chapter, the soil specimens obtained from each site (i.e., Norman, Lake Hefner, and Ardmore) were visually inspected and classified. Based on this description (i.e., mainly by color and texture), the soil specimens were put into different groups. The main purpose of this approach was to reduce the number of tests, and the problems with the soil disturbance. In this regard, the soil specimens collected from the Norman site were grouped into two soil types. Atterberg limits, compaction tests, sieve and hydrometer analyses tests were conducted on the soil specimens selected from each soil type. Table 4.1 gives the results of Atterberg limits on the soil types for each site and Table 4.2 summarizes the diffusion coefficient, initial total suction, maximum dry unit weight, and optimum moisture content test results on the compacted specimens. The compaction curves and grain size distribution plots for each soil type are provided in Appendix D and Appendix E, respectively.

4.7.1 Norman Site Diffusion Test Results on Shelby Tube Specimens

In total, eight drying diffusion coefficient tests were conducted on the soil specimens collected from the Norman site. Table 4.3 gives the initial water content, initial total suction, and diffusion coefficient parameters. The total suction measurements were conducted using either the filter paper method or the chilled-mirror psychrometer, and in some cases, both methods were employed for measuring the initial suction in the soil. The filter paper method takes at least one week for the suction equilibrium. On the other hand, the chilled-mirror device uses a small soil specimen and a sophisticated technology and measures the suction in less than 10 minutes. However, the chilled-mirror device can only reliably measure the suction values larger than

about 3.7 pF. This is a big limitation of this equipment for its wide use in engineering practice. The filter paper method measures practically the whole range of suction, but it is more reliable if the suction values are above 2 pF. The atmospheric suction in the laboratory environment was around 6 pF during the diffusion coefficient measurements. Table 4.3 gives a range of diffusivity parameters for the soils at the Norman site. These values are relatively high as compared to some of the diffusion coefficients given in the literature (Lytton et al. 2005). These high values are attributed to the highly disturbed conditions of the specimens and the presence of cracks and root fibers. The maximum to minimum ratio of the coefficients listed in Table 4.3 is about 42.

Table 4.1 Atterberg Limits Test Results on Different Soil Types of Norman, Lake Hefner, and Ardmore Sites.

Site	**Boring No.**	**Soil Segment No.**	**Soil Type**	**Depth (feet)**	**Liquid Limit (%)**	**Plastic Limit (%)**	**Plasticity Index (%)**
Norman	1	1B1	1	2.00-2.69	36.5	16.7	19.8
	2	2C1	2	4.00-4.81	36.2	18.5	17.7
Lake Hefner	1	1B1	2	2.00-2.77	37.6	23.4	14.2
Ardmore	2	2A1	1	0.00-0.90	36.0	23.6	12.4
	2	2B1	2	2.00-3.00	52.6	27.0	25.6

Table 4.2 Drying Diffusion Coefficient Test Results on Compacted Samples.

Pavement Site	Soil Type	Compacted Soil from Mixing Soil Segments	Maximum Dry Unit Weight (pcf)	Optimum Moisture Content (%)	Initial Suction (pF)*	Diffusion Coefficient, α_{dry} (cm^2/min)
Norman	1	1A1, 2A1	112.8	17.5	4.38	2.67×10^{-3}
	2	2F1, 2F2, 2H2	118.0	11.5	3.59	4.80×10^{-3}
Lake Hefner	2	1C2, 2C3, 2D1	99.0	26.0	3.53	2.80×10^{-4}
Ardmore	1	1A1, 1A2, 2A1, 2A2	105.2	14.0	4.03	8.50×10^{-4}
	2	1B2, 2B1, 2B2, 1AA1, 1AA2	102.9	18.3	3.69	7.30×10^{-4}

*From the first recorded thermocouple psychrometer reading.

Table 4.3 Norman Site, Summary of Laboratory Diffusion Coefficient Test Results

Boring No.	Soil Segment No.	Soil Type	Depth (feet)	Initial Water Content (%)	Initial Total Suction (pF)	Diffusion Coefficient, α_{dry} (cm^2/min)
1	1A3	1	1.04-1.98	9.39	4.85	1.92×10^{-3}
2	2B1	1	2.11-2.88	8.75	5.24	2.60×10^{-4}
2	2C2	2	4.81-5.42	-	4.69	7.00×10^{-4}
2	2H2	2	14.29-15.34	17.9	2.00	1.30×10^{-4}
3	3B2	1	2.90-3.75	10.3	4.53	1.03×10^{-3}
3	3C2	2	4.83-5.90	10.2	4.03	5.40×10^{-3}
4	4A1	1	0.00-0.87	11.9	4.36	1.01×10^{-3}
4	4D2	2	7.17-7.77	15.07	3.69	2.60×10^{-3}

4.7.2 Lake Hefner Site Diffusion Test Results on Shelby Tube Specimens

In total, five drying diffusion coefficient tests were conducted on the soil specimens collected from the Lake Hefner site. Table 4.4 gives the initial water content, initial total suction, and diffusion coefficient parameters. As described in the section above, the filter paper method and chilled-mirror technique were used in measuring the initial total suction in the soil specimens tested for the diffusion coefficient. As compared to the diffusivity parameters for the Norman site, the coefficients for the Lake Hefner site returned slightly larger values indicating that the unsaturated soil moisture will travel faster at the Lake Hefner site than the Norman site. The difference between the maximum and minimum diffusivity parameters at the Lake Hefner site was 2.5, which is very small.

Table 4.4 Lake Hefner Site, Summary of Laboratory Diffusion Coefficient Test Results

Boring No.	Soil Segment No.	Soil Type	Depth (feet)	Initial Water Content (%)	Initial Total Suction (pF)	Diffusion Coefficient, α_{dry} (cm^2/min)
1	1A1	2	0.00-0.80	17.44	3.01	4.00×10^{-3}
2	2C1	2	4.00-4.87	20.2	3.95	5.30×10^{-3}
2	2D2	2	6.98-7.96	16.5	3.30	5.35×10^{-3}
3	3A2	2	0.80-1.50	17.7	3.29	2.20×10^{-3}
3	3C2	2	4.50-5.45	19.8	4.01	3.20×10^{-3}

4.7.3 Ardmore Site Diffusion Test Results on Shelby Tube Specimens

In total, ten drying diffusion coefficient tests were conducted on the soil specimens collected from the Ardmore site. Table 4.5 gives the initial water content, initial total suction, and

diffusion coefficient parameters. Depending on the dryness of the soil specimens, either the filter paper method or the chilled-mirror equipment was employed for measuring the initial total suction in the soil. The diffusivity values range from 5.4×10^{-4} cm^2/min to 9.3×10^{-3} cm^2/min for the soils at the Ardmore site. The ratio between the maximum and minimum coefficients was 17. The unsaturated soil diffusion coefficients for the Ardmore site are in the same range as the coefficients for the Norman site. As described previously, the soil specimens from the Ardmore site were also highly disturbed with significant amount of shrinkage cracks and root fibers.

Table 4.5 Ardmore Site, Summary of Laboratory Diffusion Coefficient Test Results

Boring No.	Soil Segment No.	Soil Type	Depth (feet)	Initial Water Content (%)	Initial Total Suction (pF)	Diffusion Coefficient, α_{dry} (cm^2/min)
1	1B1	2	2.00-2.80	14.3	4.71	1.98×10^{-3}
3	3C2	3	4.90-6.00	20.8	4.10	6.11×10^{-3}
4	1BB2	2	2.50-3.40	18.6	4.55	4.25×10^{-3}
4	1CC1	2	4.00-4.88	18.7	4.33	9.30×10^{-3}
5	2BB2	2	2.90-4.00	19.4	3.58	6.50×10^{-4}
5	2CC2	2	4.86-5.86	17.2	4.77	7.80×10^{-4}
6	3AA2	2	0.10-1.10	25.6	3.98	2.06×10^{-3}
6	3DD1	2	6.00-6.50	21.4	4.22	9.70×10^{-4}
7	4AA2	2	0.95-2.00	24.4	3.45	5.40×10^{-4}
7	4DD3	2	6.85-7.50	12.3	5.26	5.90×10^{-4}

The details of all the diffusion test results, including the input parameters and the relationship between the measured suction values and theoretical suction predictions, are summarized in Appendix F. These values are still being evaluated in the accompanying on-going research project for the analytical and numerical models for predicting the suction and tensile stress profiles in these soils. Chapter 5 describes these models and makes some preliminary predictions.

5 SUCTION AND TENSILE STRESS PROFILES

Simple and practical (yet realistic) methods are needed to analyze and model the longitudinal drying shrinkage problems in pavemet subgrades. These methods must also consider the principles of unsaturated soil mehanics. Development of a simple analytical model for predicting soil suction distribution beneath a pavement structure and calculating the corresponding tensile stresses in the soil has been an important component of this study. It is believed that the moisture content-based stress analyses model proposed by Sumarac (2004) and the suction distribution model given by Mitchell (1979) can be modified into a practical approach for analyzing the shrinkage problem in high plastic soils. The model parameters for these appraoches can be determined in the laboratory and estimated using basic soil index test results.

5.1 Soil Suction Profiles

The effect of low relative humidity on the ground surface (i.e., soil drying) on the state of suction in the soil can be determined by means of obtaining a solution of the diffusion equation for a soil profile subjected to a constant state of suction at the surface. The one-dimensional partial differential equation describing the moisture diffusion problem in response to suction change is given as:

$$\alpha_{dry}\nabla^2 u = \frac{\partial u}{\partial t} \tag{5.1}$$

where, α_{dry} is the unsaturated diffusivity parameter for a drying soil, u is the total suction, and t is the time. If a soil profile of a drying diffusion coefficient (α_{dry}) is initially at a constant suction (u_o) and is subjected to a state of suction (u_f) at the surface, the solution of the diffusion equation is as follows (Mitchell 1979):

$$u\ x,t\ = u_0 + (u_f - u_0)\ (1 - erf\frac{x}{2\ \overline{\alpha_{dry}t}}) \quad (5.2)$$

where, *x* is the depth and *erf* is the error function. Equation 5.2 can predict suction profiles in a drying shrinking soil using a laboratory determined soil parameter (α_{dry}) and initial and surface suction values which depend on the climate of the region. The initial suction can be predicted from the Thornthwaite Moisture Index (TMI) maps or it can be measured in the field.

Figure 5.1 depicts several suction profiles that consider typical soil and climatic parameters that were obtained in this study. The unsaturated diffusivity parameter, α_{dry} is equal to 0.001 cm^2/sec (which is on the very high side of the values measured in this study) and equilibrium initial suction is considered to be 3.5 pf. The soil surface is then exposed to different levels of relative humidity (i.e., suction) as shown in Figure 5.1.

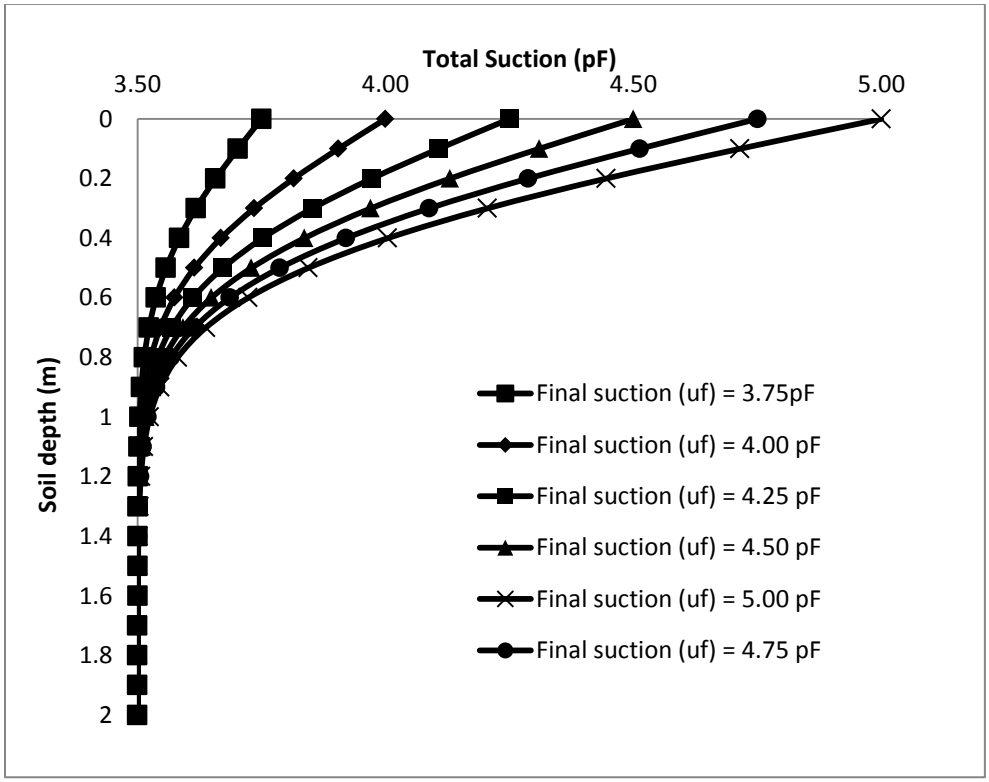

Figure 5.1 Variation of suction profiles for different final suctions using Equation 5.2

As described in the previous chapters, measurement of the unsaturated diffusivity coefficient in the laboratory is one of the critial component of this study. For all the three sites (i.e., Norman, Lake Hefner, and Ardmore), relatively wide ranges of the diffusivity parameters were measured in the lab on the Shelby tube and compacted soil specimens. The effects of the diffusion coefficient on the suction profiles is significant and typical ranges are given in Figure 5.2.

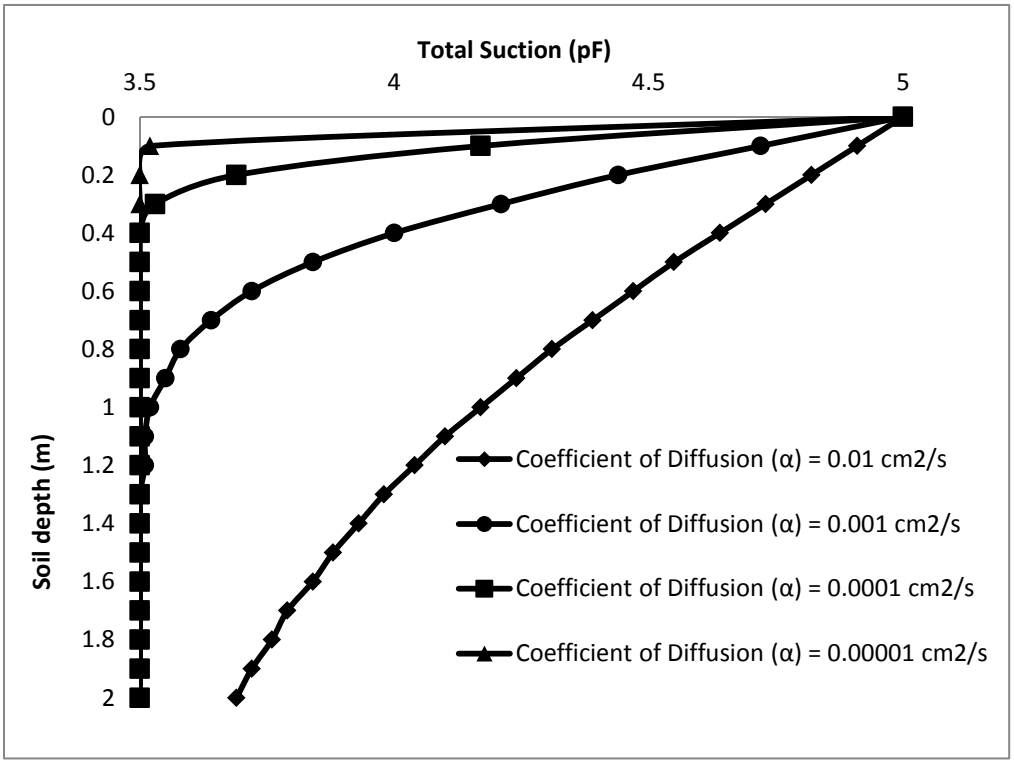

Figure 5.2 Variation of Suction Profiles for different diffusion coefficients.

5.2 Tensile Stress Profiles in Drying Shrinkage Soils

The longitudinal shrinkage cracking along the pavement shoulders is controlled by the suction profiles and corresponding tensile stresses in the soil. The suction profile with depth in the pavement section can be determined by taking periodic suction measurements with depth or it can be predicted using Equation 5.2 as proposed by Mitchell (1979) for modeling the effect of

garden watering on the ground surface. This equation can be adopted for modeling the suction profile in the drying soil using the drying unsaturated diffusion coefficient as well.

Tensile stresses in subgrade soils develop in response the suction profiles in the soil. Sumarac (2004) presented an analytical approach for shrinkage crack analysis using a water content change approach. In the current study, the Sumarac (2004) water content based model was modified for the suction stress state in unsaturated soils. The model considers a semi-infinite elastic soil medium with uniform initial distribution of suction in the soil. The movement of moisture is in response to the equilibrium initial suction and the suction imposed at the ground surface, and the rate of moisture movement is controlled by the unsaturated diffusivity parameter. The modified equation is given as:

$$\sigma_x = \frac{E\gamma_h}{1-\nu}(u_f - u_o)\left(1 - erf\frac{x}{2\sqrt{\alpha_{dry}t}}\right) \quad (5.3)$$

where, σ_x is the tensile stress in the soil, E is the modulus of elasticity, ν is the Poisson's ratio, and γ_h is the suction compression index. While E and ν can be found in the literature for various types of soils, γ_h can be estimated from basic soil index parameters (Lytton et al. 2005). Figure 5.3 gives the tensile stress profiles using Equation 5.3. The soil is drying from an initial and equilibrium suction profile of 3.5 pF to various surface suction conditions as shown in Figure 5.3. For the analysis, the suction compression index (γ_h), drying diffusion coefficient (α_{dry}), elastic modulus (E), and Poisson's ratio values were taken as 0.01, 0.001 cm^2/sec, 7 MPa, and 0.3, respectively. It should be pointed out that these tensile stresses may not be mobilized in the field because development of those stresses in the soil also depend on the fracture toughness of the material (i.e., tensile strength of the material). The test results obtained in this study are being used and evaluated in the proposed analytical models. These aspects of the study are currently

being conducted in the accompanying on-going research project and will be included in the comprehensive final report to ODOT.

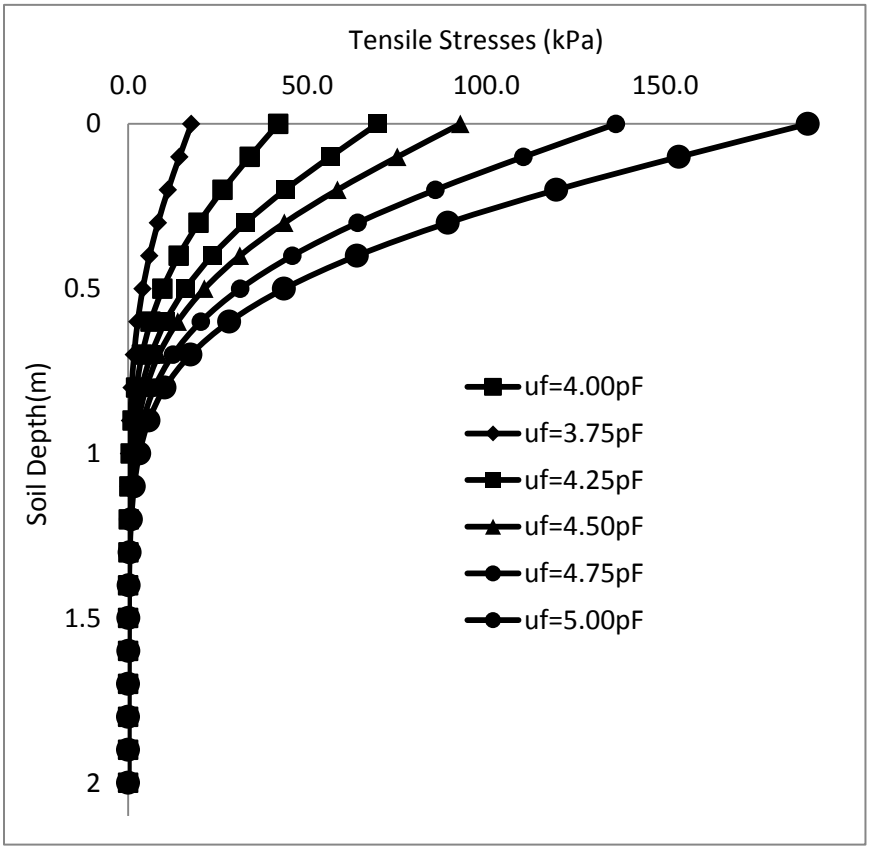

Figure 5.3 Tensile Stress Profiles in Response Suction Variations

THIS PAGE IS INTENTIONALLY LEFT BLANK

6. CONCLUSIONS

In recent years, a significant effort has been directed to better analyze the ground and climate interactions as applicable to a range of transportation structures. Drying shrinkage cracking in the pavement structure has been a major problem in Oklahoma. In many cases, this type of cracking initiates in the drying subgrade soil and reflects from the highly plastic subgrade through the pavement structure. The relatively impermeable pavement surface has a significant impact on the formation of the non-uniform moisture profiles. The mechanism of crack development, therefore, is rooted in the moisture (suction) variation in the shrinking high PI subgrade soil. The gradients of moisture variation, togther with the soil volume change characteristics, determine the tensile stress distribution and shrinkage crack initiation.

The current study investigated the longitudinal drying shrinkage problems in pavement subgrade soils at three sites in Oklahoma. Two of the sites located in Norman and Oklahoma City are bike trails and the third site is along the Interstate Highway I-35 in Ardmore. The soil specimens collected from these sites were tested for the basic index properties as well as suction and unsaturated diffusivity measurements. Various ranges of the test results have been implemented in a suction profile and tensile stress prediction models for evaluating the typical suction changes and the corresponding tensile stresses in subgrade soils. This part of the study is currently being conducted further in the accompanying on-going research project and the results will be included in the comprehensive final report to ODOT.

THIS PAGE IS INTENTIONALLY LEFT BLANK

REFERENCES

Ayad, R., J.M. Konrad, and M. Soulie (1997). Desiccation of a Sensitive Clay: Application of the Model CRACK. Canadian Geotechnical Journal, V 34, pp. 943-951.

Bulut, R. and E. C. Leong (2008). Indirect Measurement of Suction. Special Issue on Laboratory and Field Testing of Unsaturated Soils. Journal of Geotechnical and Geological Engineering, Vol. 26, No. 6, pp. 633-644.

Bulut R., R.L. Lytton, W.K. Wray (2001). Soil Suction Measurements by Filter Paper. ASCE Geotechnical Special Publication No. 115, pp. 243–261.

Bulut R., S.M. Hineidi, and B. Bailey (2002). Suction Measurements—Filter Paper and Chilled Mirror Psychrometer. Proceedings of the Texas Section American Society of Civil Engineers, Fall Meeting, Waco, October 2-5, 2002, CD-ROM.

Crockford, W. W. and D.N. Little (1987). Tensile Fracture and Fatigue of Cement-Stabilized Soil. Journal of Transportation Engineering, Vol. 113, No. 5, American Society of Civil Engineers (ASCE), pp. 520-537.

Fredlund D.G., and N.R. Morgenstern (1977). Stress State Variables for Unsaturated Soils. Journal of Geotechnical Engineering, Vo. 103, pp. 447–466.

Harison, J. A., B.O. Hardin, and K. Mahboub (1994). Fracture Toughness of Compacted Cohesive Soils Using Ring Test. Journal of Geotechnical Engineering, Vol. 120, No. 5, pp. 872-891.

Jayatilaka, R., D.A. Gay, R.L. Lytton, and W.K. Wray (1993). Effectiveness of Controlling Pavement Roughness due to Expansive Clays with Vertical Moisture Barriers. FHWA/TX-92/1165-2F Research Report, Texas Transportation Institute, College Station, Texas.

Kodikara, J.K., S.L. Barbour, and D.G. Fredlund (2002). Structure Development in Surficial Heavy Clay Soils: A Synthesis of Mechanisms. Australian Geomechanics, Vol. 37, No. 3, pp. 25–40.

Konrad, J.-M., and R. Ayad (1997). Desiccation of a Sensitive Clay: Field Experimental Observations. Canadian Geotechnical Journal, Vol. 34, pp. 929-943.

Long, X. (2006). Prediction of Shear Strength and Vertical Movement due to Moisture Diffusion through Expansive Soils. Ph.D. Dissertation. Texas A&M University, College Station, Texas.

Luo, R. (2007). Minimizing Longitudinal Pavement Cracking due to Subgrade Shrinkage. Ph.D. Dissertation. University of Texas-Austin, Texas.

Luo, R. and J.A. Prozzi (2009). Combining Geogrid Reinforcement and Lime Treatment to Control Dry Land Longitudinal Cracking. Transportation Research Record: Journal of the Transportation Research Board, Volume 2104, pp. 88-96.

Luo, R. and J.A. Prozzi (2008). Development of Longitudinal Cracks on Pavement over Shrinking Subgrade. Transportation Research Board 87th Annual Meeting, Paper #08-1034, CD-ROM.

Lytton, R. L., C. Aubeny, and R. Bulut (2005). Design Procedure for Pavements on Expansive Soils, Research Report FHWA/TX-05/0-4518-1, Vol. 1, Texas Transportation Institute, Texas A&M University, College Station, Texas.

Mabirizi, D. and R. Bulut (2010). A Unified Testing Method for Measuring Unsaturated Soil Drying and Wetting Diffusion Coefficients in Laboratory, Transportation Research Record: Journal of the Transportation Research Board, No. 2170, Transportation Research Board of the National Academies, Washington, D.C., pp. 109-118.

Mitchell, P. W. (1979). "The structural analysis of footings on expansive soil." Kenneth W.G. Smith and Associates Research Report No. 1, pp. 1-159, Newton, South Australia.

Nevels, J.B. (2006). An Evaluation of Horizontal Membrane Barriers in Controlling Longitudinal Cracking. ASCE Special Publication No. 147, pp. 269-280.

Nuhfer, E.B., R.J. Proctor, and N. Moser (1993). The Citizen's Guide to Geologic Hazards. AIPG Press: Arvada, CO; p 134.

Puppala, A.J., T. Manosuthhikji, L. Hoyos, and S. Nazarian (2009). Moisture and Suction in Clay Subgrades Prior to Initiation of Pavement Cracking, TRB 88th Annual Meeting Compendium of Papers DVD, Transportation Research Board Annual Meeting 2009 Paper #09-1522, 13p.

Sabnis, A., I. Abdallah, S. Nazarian, and A.J. Puppala (2010). Development of Shrinkage Model for Clays Based on Moisture Variation. Experimental and Applied Modeling of Unsaturated Soils, Proceedings of Sessions of GeoShanghai 2010 International Conference, June 3-5, Shanghai, pp. 166-172.

Sumarac, D. (2004). Moisture Diffusion Induced Soil Cracking. The First International Conference on Computational Mechanics (CM'04), Belgrade, Serbia and Montenegro, November 15-17, 2004, pp. 1-13.

Thornthwaite, C.W. (1948). An Approach Toward a Rational Classification of Climate. Geographical Review, Vol. 38, pp. 55-94.

Thornthwaite, C.W. and J.R. Mather (1955). The Water Balance. *Publication of Climatology*, Laboratory of Climatology, Vol. 8, No. 1, 104 p.

Witczak, M.W., C.E. Zapata, and W.N. Houston (2006). Models Incorporated into the Current Enhanced Integrated Climatic Model for Used in Version 1.0 of the ME-PDG. NCHRP 9-23 Project Report, Arizona State University, Tempe, Arizona.

Wray, W.K. and K.T. Meyer (2004). Expansive Clay Soil… A Widespread and Costly GeoHazard. GeoStrata, ASCE GeoInstitute. Vol. 5, No. 4, October, 2004. pg. 24-25, 27-28.

APPENDICES

APPENDIX A

Table A1. Norman Site, Boring 1, Soil Description Based on Visual Inspection

Shelby Tube	Soil Segment	Depth (feet)	Soil Description	Soil Type
1A	1A1	0 to 0.83	Light to dark brown, root fibers close to surface, significant amount of sample disturbance and cracking. Only in 1B1 and 1B2, there are some iron stains.	Type 1
	1A2	0.83 to 1.04		
	1A3	1.04 to 1.98		
1B	1B1	2.0 to 2.69		
	1B2	2.69 to 3.32		

Table A2. Norman Site, Boring 2, Soil Description Based on Visual Inspection

Shelby Tube	Soil Segment	Depth (feet)	Soil Description	Soil Type
2A	2A1	0 to 0.75	Light brown 2A1 to dark brown 2A5, root fibers close to the surface. Only in 2A1, significant deep cross-sectional crack almost dividing it into two halves. Only in 2A1 and 2A2, there are some iron stains.	Type 1
	2A2	0.75 to 1.07		
	2A3	1.07 to 1.37		
	2A4	1.37 to 1.71		
	2A5	1.71 to 1.90		
2B	2B1	2.11 to 2.88	Light brown, significant disturbance, few small white aggregates.	Type 1
	2B2	2.88 to 3.19		
	2B3	3.19 to 3.5		
2C	2C1	4.0 to 4.81	Red in color, some disturbance.	Type 2
	2C2	4.81 to 5.42		
2D	2D1	6.0 to 6.63		
	2D2	6.63 to 7.16		
	2D3	7.16 to 8		
2E	2E1	8.0 to 9.02	Red in color, partial disturbance, hair cracks in the undisturbed part.	
	2E2	9.02 to 10	Red in color, minimal disturbance.	
2F	2F1	10.0 to 10.55	Red in color, almost no disturbance, moist. For 2F1 only, surface along the length of the specimen is darker in color than the bottom end. For 2F2 only, the specimen has been broken into two pieces while unwrapping. For 2H3 only, specimen already broken into 2 pieces.	
	2F2	10.55 to 11.35		
	2F3	11.35 to 11.95		
2G	2G1	12.0 to 12.72		Type 2
	2G2	12.72 to 13.34		
	2G3	13.34 to 14		
2H	2H1	14.0 to 14.29		
	2H2	14.29 to 15.34		
	2H3	15.34 to 15.75		
	2H4	15.75 to 16		
2I	2I1	16.0 to 16.5	Red in color, specimen is very wet.	
	2I2	16.5 to 17.55	Red in color, specimen is moist, top part is separated (2 inch), bottom part is separated (2 inch), middle part is broken into 2 halves.	Type 2
	2I3	17.55 to 18	Red in color, specimen is moist, few hair cracks.	

Table A3. Norman Site, Boring 3, Soil Description Based on Visual Inspection

Shelby Tube	Soil Segment	Depth (feet)	Soil Description	Soil Type
3A	3A1	0.0 to 1.1	Entirely disturbed (collapsed), brown in color, root fibers.	Type 1
	3A2	1.1 to 2.0	Disturbed, brown in color, root fibers.	
3B	3B1	2.0 to 2.9	Slightly disturbed, fallen parts from top, light brown in color, broken into 2 halves while unwrapping.	
	3B2	2.9 to 3.75	Light brown in color, black spots, slightly disturbed.	
3C	3C1	4.0 to 4.83	Red in color for 3C1 and 3C2. Top surface of 3C1 is disturbed (fallen particles) and dark brown in color. Some disturbance for the rest of 3C1 and all 3C2.	Type 2
	3C2	4.83 to 5.90		
3D	3D1	6.0 to 7.15	Red in color (whole push-tube). For 3D1, length of 6 cm is separated from rest of segment. Fallen particles from top end of 3D1, minimal disturbance for rest of 3D1. Top part of 3D2 is totally disturbed, rest of 3D2 is undisturbed, moisture appears.	
	3D2	7.15 to 8		
3E	3E1	8.0 to 8.95	Red in color. 3E1 is partially disturbed. Top part of 3E2 is separated, rest of 3E2 is undisturbed.	
	3E2	8.95 to 9.85		
3F	3F1	10.0 to 10.97	Red in color, slightly disturbed in general, cross-sectional crack in the middle of 3F2.	
	3F2	10.97 to 11.60		
3G	3G1	12.0 to 12.91	Red in color, undisturbed, one visible crack near top of 3G2.	
	3G2	12.91 to 13.78		
3H	3H1	14.0 to 14.07	Red in color, 3H1 disturbed from bottom end, 3H2 highly disturbed.	
	3H2	14.07 to 15.90		
3I	3I1	16.0 to 16.75	Red in color, highly disturbed, cross-section is not uniform along 3I1, cross-sectional crack in bottom of 3I1, 3I2 already broken into 4 pieces.	
	3I2	16.75 to 17.69		

Table A4. Norman Site, Boring 4, Soil Description Based on Visual Inspection

Shelby Tube	Soil Segment	Depth (feet)	Soil Description	Soil Type
4A	4A1	0 to 0.87	Very dark brown, root fibers, few small cracks.	Type 1
	4A2	0.87 to 1.62	Brown in color, traces of root fibers, few thin cracks.	
4B	4B1	2.0 to 3.0	Brown in color, highly disturbed, top part of 4B1 is separated.	
	4B2	3.0 to 3.25		
	4B3	3.25 to 3.87		
	4B4	3.87 to 4.0		
4C	4C1	4.0 to 5.0	Red in color, top part of 4C1 is brown in color, cracks in general, top part of 4C1 is highly disturbed, top part of 4C2 is separated.	Type 2
	4C2	5.0 to 5.95		
4D	4D1	6.0 to 7.17	Red in color. For 4D1 only, root fibers 4D1, cracked. For 4D2 only, minimum cracks, top part is separated.	
	4D2	7.17 to 7.77		
4E	4E1	8.0 to 9.0	Red in color, slightly disturbed.	
	4E2	9.0 to 9.77		
4F	4F1	10.0 to 11.0	Red in color, cracked and disturbed.	
	4F2	11.0 to 12.0	Red in color, undisturbed.	
4G	4G1	12.0 to 13.2	Red in color, slightly disturbed.	
	4G2	13.2 to 14.0		
4H	4H1	14.0 to 15.0	Red in color, disturbed (squeezed).	
	4H2	15.0 to 15.73		
4I	4I1	16.0 to 17.0	Red in color, highly disturbed.	
	4I2	17.0 to 17.85		

APPENDIX B

Table B1. Lake Hefner Site, Boring 1, Soil Description Based on Visual Inspection

Shelby Tube	Soil Segment	Depth (feet)	Soil Description	Soil Type
1A	1A1	0 to 0.8	Dark brown in color, disturbed. For 1A1 only, root fibers, slightly disturbed.	Type 1
	1A2	0.8 to 1.37		
	1A3	1.37 to 1.92		
1B	1B1	2.0 to 2.77	Light red, highly disturbed, similar to tennis court soil.	Type 2
	1B2	2.77 to 3.55		
	1B3	3.55 to 3.98		
1C	1C1	4.0 to 4.70	Dark red, disturbed.	
	1C2	4.70 to 5.58		
	1C3	5.58 to 5.99		
1D	1D1	6.0 to 6.99	Dark red, top part is greenish, highly disturbed.	
	1D2	6.99 to 7.81	Dark red, disturbed.	
1E	1E1	8.0 to 0.74	Dark red, slightly disturbed.	

Table B2. Lake Hefner Site, Boring 2, Soil Description Based on Visual Inspection

Shelby Tube	Soil Segment	Depth (feet)	Soil Description	Soil Type
2A	2A1	0 to 1.0	Root fibers, dark brown, disturbed	Type 2
	2A2	1.0 to 1.86	Red, traces of root fibers, disturbed.	
2B	2B1	2.0 to 2.94	Light red, traces of root fibers, disturbed.	
	2B2	2.94 to 3.64		
2C	2C1	4.0 to 4.87	Red, disturbed.	
	2C2	4.87 to 4.97		
	2C3	4.97 to 5.95		
2D	2D1	6 to 6.98		
	2D2	6.98 to 7.96		
2E	2E1	8 to 8.82		

Table B3. Lake Hefner Site, Boring 3, Soil Description Based on Visual Inspection

Shelby Tube	Soil Segment	Depth (feet)	Soil Description	Soil Type
3A	3A1	0 to 0.80	Living insects, brown, root fibers, disturbed.	Type 2
	3A2	0.80 to 1.50	Reddish brown, traces of root fibers, disturbed.	
3B	3B1	1.5 to 2.5	Light orange/red, traces of root fibers, disturbed.	
	3B2	2.5 to 3.35		
3C	3C1	3.5 to 4.5	Light orange/red, disturbed.	
	3C2	4.5 to 5.45	Red, slightly disturbed.	
3D	3D1	5.5 to 6.38	Dark red, highly disturbed.	
3E	3E1	–	Specimen not received.	

APPENDIX C

Table C1. Ardmore Site, Boring 1, Soil Description Based on Visual Inspection

Shelby Tube	Soil Segment	Depth (feet)	Soil Description (Visual Inspection)	Soil Type
1A	1A1	0 to 0.95	Root fibers, black, slightly disturbed.	Type 1
	1A2	0.95 to 1.95	Root fibers, black, disturbed.	
1B	1B1	2.0 to 2.80	Traces of root fibers, brownish, disturbed.	Type 2
	1B2	2.80 to 3.57	Root fibers, brownish, disturbed.	

Table C2. Ardmore Site, Boring 2, Soil Description Based on Visual Inspection

Shelby Tube	Soil Segment	Depth (feet)	Soil Description (Visual Inspection)	Soil Type
2A	2A1	0 to 0.90	Root fibers, black, disturbed.	Type 1
	2A2	0.90 to 1.90	Root fibers, black with brown stains, disturbed.	
2B	2B1	2.0 to 3.0	Root fibers traces, brownish, disturbed.	Type 2
	2B2	3.0 to 3.45	Light brown, highly disturbed/collapsed.	

Table C3. Ardmore Site, Boring 3, Soil Description Based on Visual Inspection

Shelby Tube	Soil Segment	Depth (feet)	Soil Description (Visual Inspection)	Soil Type
3A	3A1	0 to 1.1	Root fibers, black, disturbed, moisture appears.	Type 1
	3A2	1.1 to 1.85	Brownish, cracked, moisture appears.	Type 2
3B	3B1	2.0 to 2.90	Brownish, disturbed, sample cross-section is not fully cylindrical.	
	3B2	2.90 to 3.45	Dark brown, slightly disturbed.	
	3B3	3.45 to 4.0		
3C	3C1	4.0 to 4.90	Light black, highly disturbed.	Type 3
	3C2	4.90 to 6.0	Light black, undisturbed.	

Table C4. Ardmore Site, Boring 4, Soil Description Based on Visual Inspection

Shelby Tube	Soil Segment	Depth (feet)	Soil Description (Visual Inspection)	Soil Type
1AA	1AA1	0 to 1.0	Root fibers, brownish, slightly disturbed.	Type 2
	1AA2	1.0 to 2.0	Brownish, disturbed.	
1BB	1BB1	2.0 to 2.5	Root fibers, brownish, disturbed.	
	1BB2	2.5 to 3.4	Dark brown, undisturbed, cracked, small white aggregates.	
	1BB3	3.4 to 3.5	Brown, hollow.	
	1BB4	3.5 to 3.90	Dark brown, undisturbed.	
1CC	1CC1	4.0 to 4.88	Dark brown, partially disturbed.	
	1CC2	4.88 to 5.80	Brown, undisturbed, few cracks.	
	1CC3	5.80 to 6.0		
1DD	1DD1	6.0 to 6.50	Brown, partially disturbed, separated.	
	1DD2	6.50 to 7.50	Brown, disturbed.	
	1DD3	7.50 to 8.0	Brown, undisturbed.	

Table C5. Ardmore Site, Boring 5, Soil Description Based on Visual Inspection

Shelby Tube	Soil Segment	Depth (feet)	Soil Description (Visual Inspection)	Soil Type
2AA	2AA1	0 to 0.90	Root fibers, brown, undisturbed	Type 2
	2AA2	0.90 to 1.90	Brown, undisturbed, small white aggregates.	
	2AA3	1.90 to 2.0	Brown, undisturbed	
2BB	2BB1	2.0 to 2.90	Black, partially disturbed, small white aggregates.	Type 1
	2BB2	2.90 to 4.0	Dark brown, undisturbed, small white aggregates.	Type 2
2CC	2CC1	4.0 to 4.86	Root fibers, brown, partially disturbed.	
	2CC2	4.86 to 5.86	Brown, undisturbed.	
	2CC3	5.86 to 6.0		
2DD	2DD1	6.0 to 6.5	Brown to light black, disturbed, red particles.	Type 3
	2DD2	6.5 to 7.10	Brownish, undisturbed.	Type 2
	2DD3	7.10 to 7.50		
	2DD4	7.50 to 8.0	Brownish, disturbed.	

Table C6. Ardmore Site, Boring 6, Soil Description Based on Visual Inspection

Shelby Tube	Soil Segment	Depth (feet)	Soil Description (Visual Inspection)	Soil Type
3AA	3AA1	0 to 0.1	Root fibers, brown, undisturbed.	Type 2
	3AA2	0.1 to 1.1	Root fibers, brown with black stains, undisturbed.	
3BB	3BB1	2.0 to 3.15	Black, disturbed, small white aggregates.	Type 1
	3BB2	3.15 to 3.85	Dark brown, undisturbed, cracked, small white aggregates.	Type 2
3CC	3CC1	4.0 to 4.95	Root fibers, brown, disturbed, small white aggregates.	
	3CC2	4.95 to 6.0	Brown, partially disturbed, small white aggregates.	
3DD	3DD1	6.0 to 6.50	Brown, undisturbed.	
	3DD2	6.50 to 7.45	Brown, undisturbed, separated, red particles.	
	3DD3	7.45 to 8.0	Brown, disturbed, red particles.	

Table C7. Ardmore Site, Boring 7, Soil Description Based on Visual Inspection

Shelby Tube	Soil Segment	Depth (feet)	Soil Description (Visual Inspection)	Soil Type
4AA	4AA1	0 to 0.95	Living insects, root fibers, brown, disturbed.	Type 2
	4AA2	0.95 to 2.0	Dark brown, partially disturbed.	
4BB	4BB1	2.0 to 3.0	Brownish, disturbed, small white aggregates.	
	4BB2	3.0 to 4.0		
4CC	4CC1	4.0 to 4.85	Root fibers, brownish, disturbed, small white aggregates.	
	4CC2	4.85 to 5.5	Brown, undisturbed.	
	4CC3	5.5 to 6.0	Brown, disturbed.	
4DD	4DD1	6.0 to 6.50	Brown, undisturbed, cracked.	
	4DD2	6.50 to 6.85	Brown, undisturbed.	
	4DD3	6.85 to 7.50	Brownish, undisturbed.	
	4DD4	7.50 to 8.0	Brownish, disturbed, small white aggregates.	

APPENDIX D

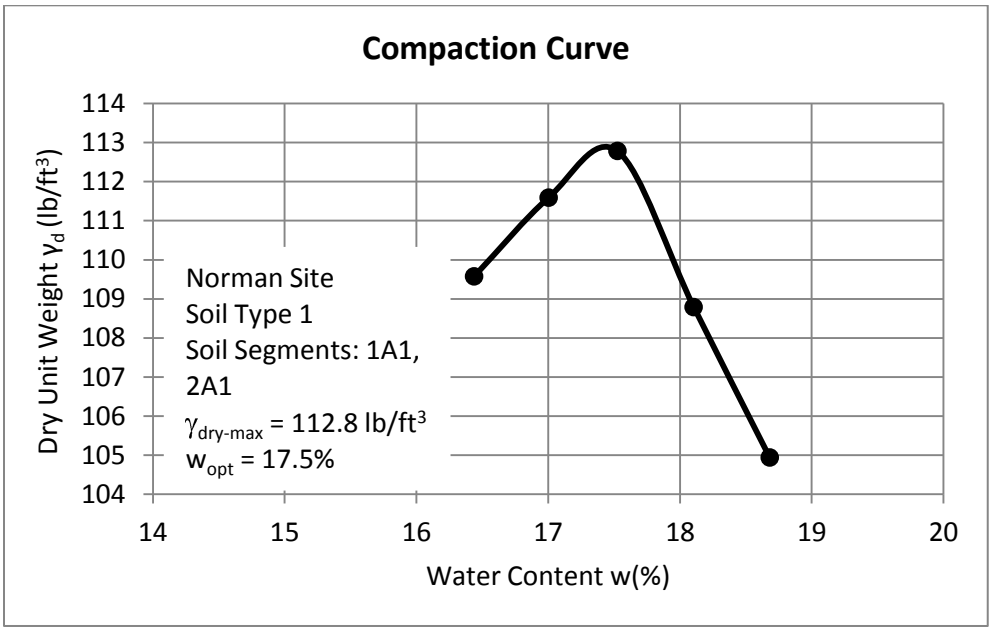

Figure D1. Relation between the dry unit weight and the water content for the soil from segments 1A1, 2A1 of type 1 of Norman Site

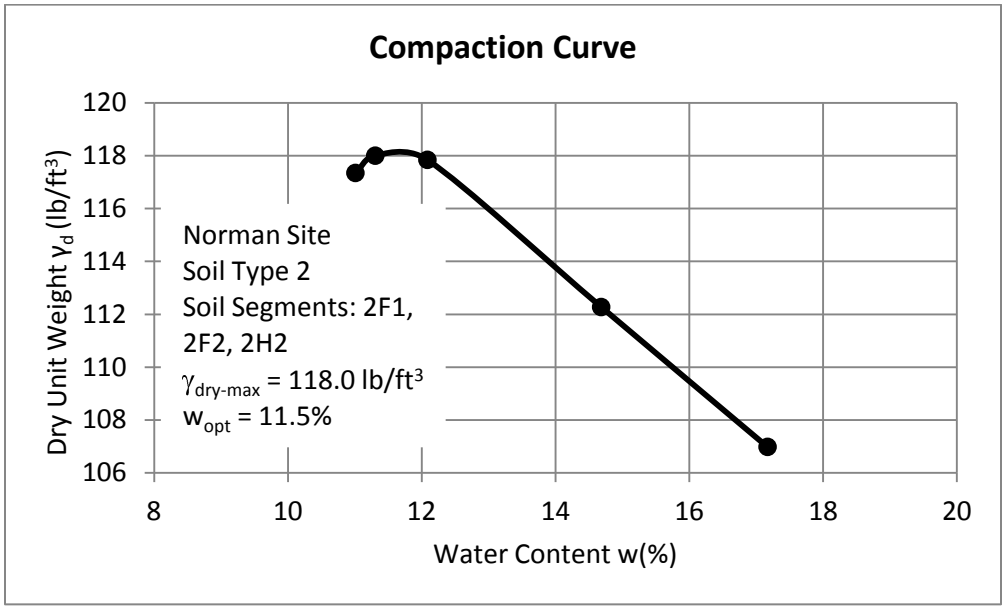

Figure D2. Relation between the dry unit weight and the water content for the soil from soil segments 2F1, 2F2, 2H2 of type 2 of Norman site

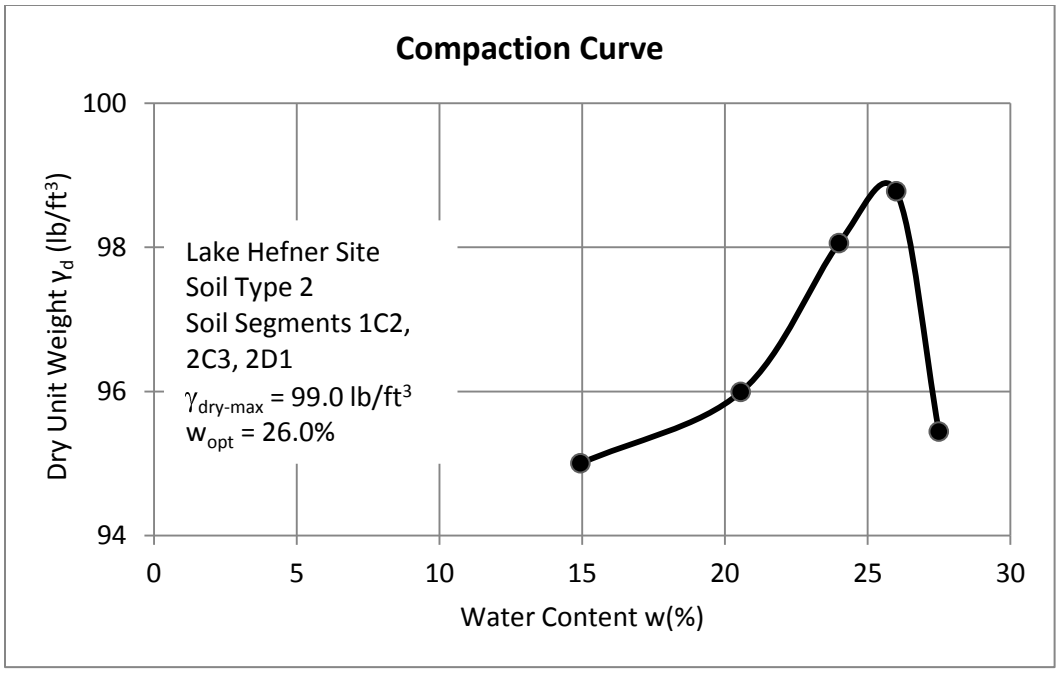

Figure D3. Relation between the dry unit weight and the water content for the soil from soil segments 1C2, 2C3, 2D1 of type 2 of Lakehefner site

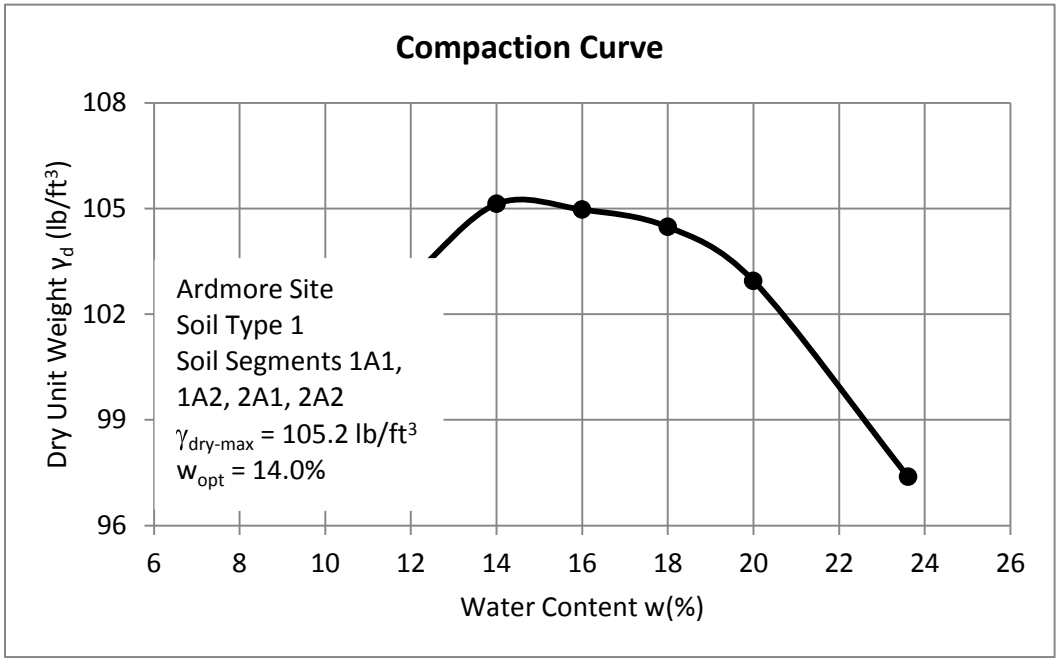

Figure D4. Relation between the dry unit weight and the water content for the soil from soil segments 1A1, 1A2, 2A1, 2A2 of type 2 of Ardmore site

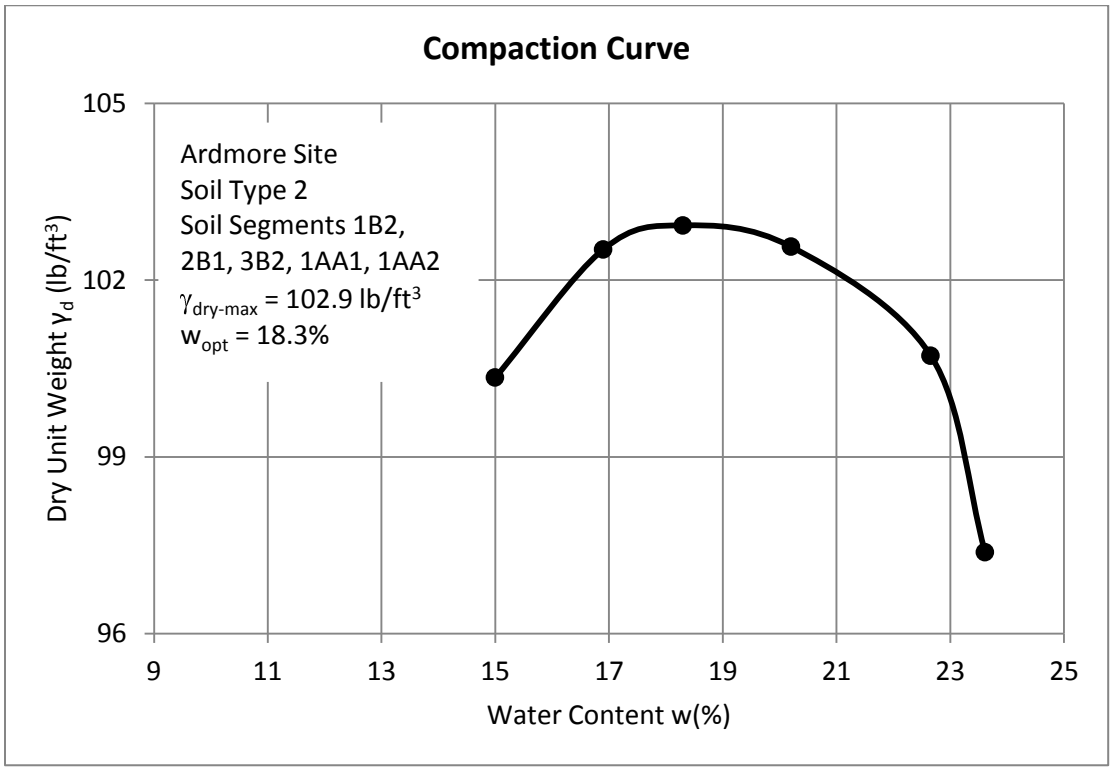

Figure D5. Relation between the dry unit weight and the water content for the soil from soil segments 1B2, 2B1, 3B2, 1AA1, 1AA2 of type 2 of Ardmore site

THIS PAGE IS INTENTIONALLY LEFT BLANK

APPENDIX E

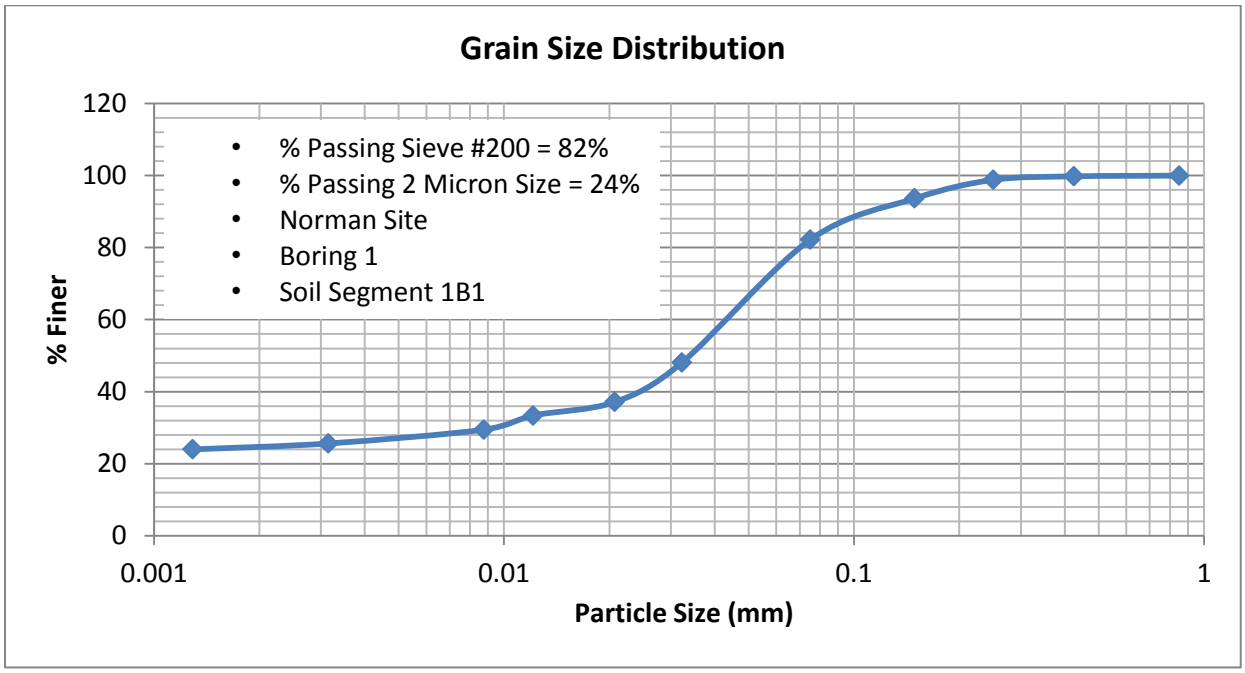

Figure E1. Grain Size Distribution curve for the soil from boring 1, Soil segment 1B1 of Norman site

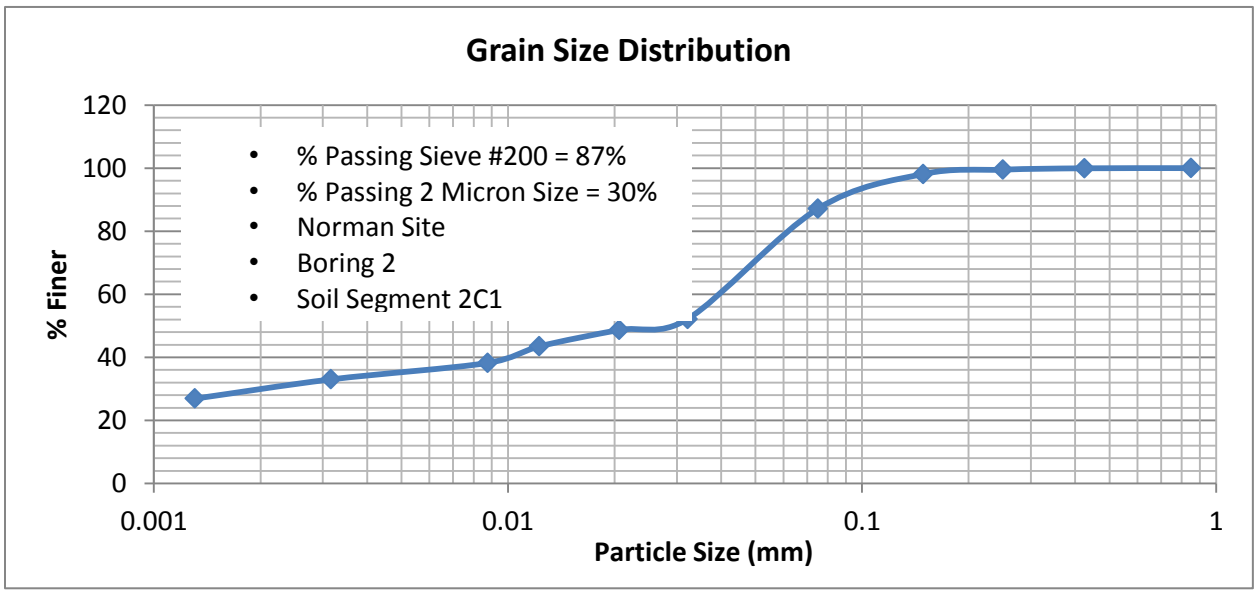

Figure E2. Grain Size Distribution curve for the soil from boring 1, Soil segment 2C1 of Norman site

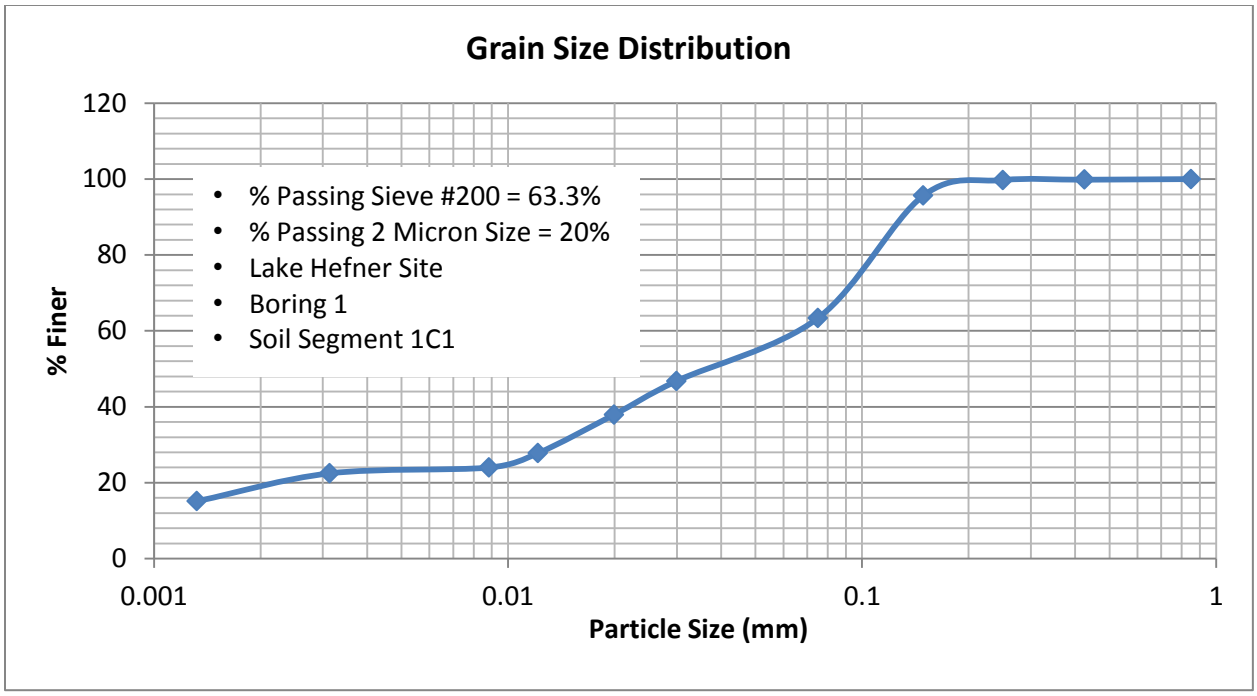

Figure E3. Grain Size Distribution curve for the soil from boring 1, Soil segment 1C1 of Lakehefner site

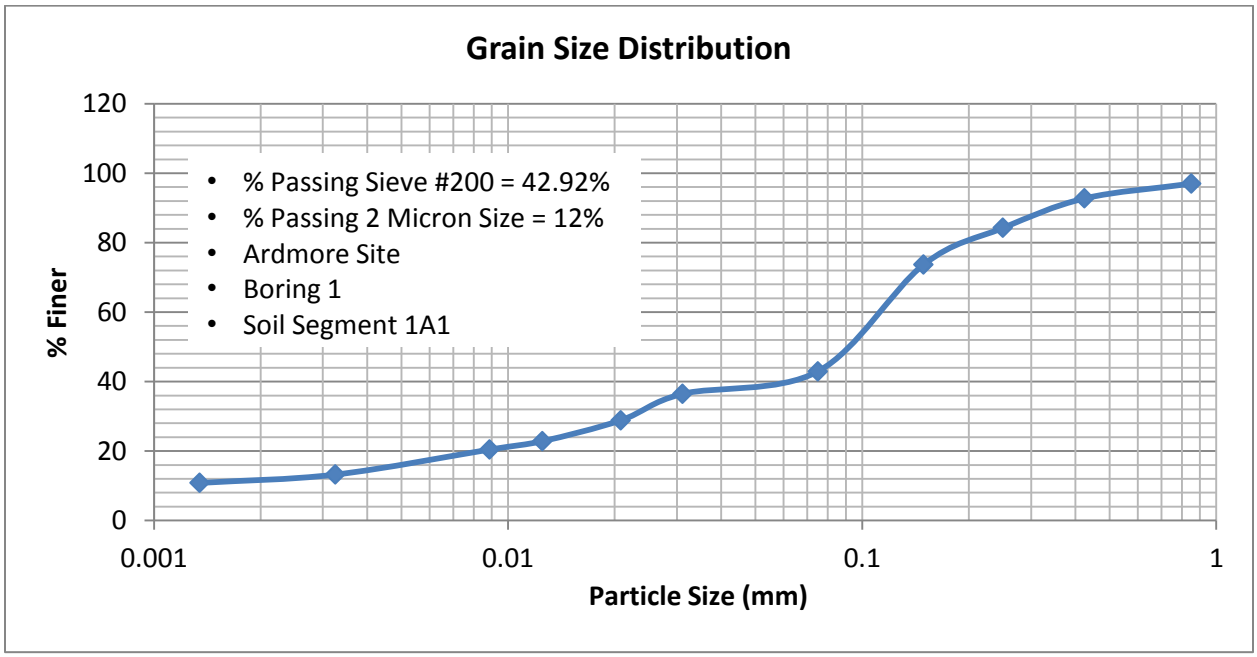

Figure E4. Grain Size Distribution curve for the soil from boring 1, Soil segment 1A1 of Ardmore Site

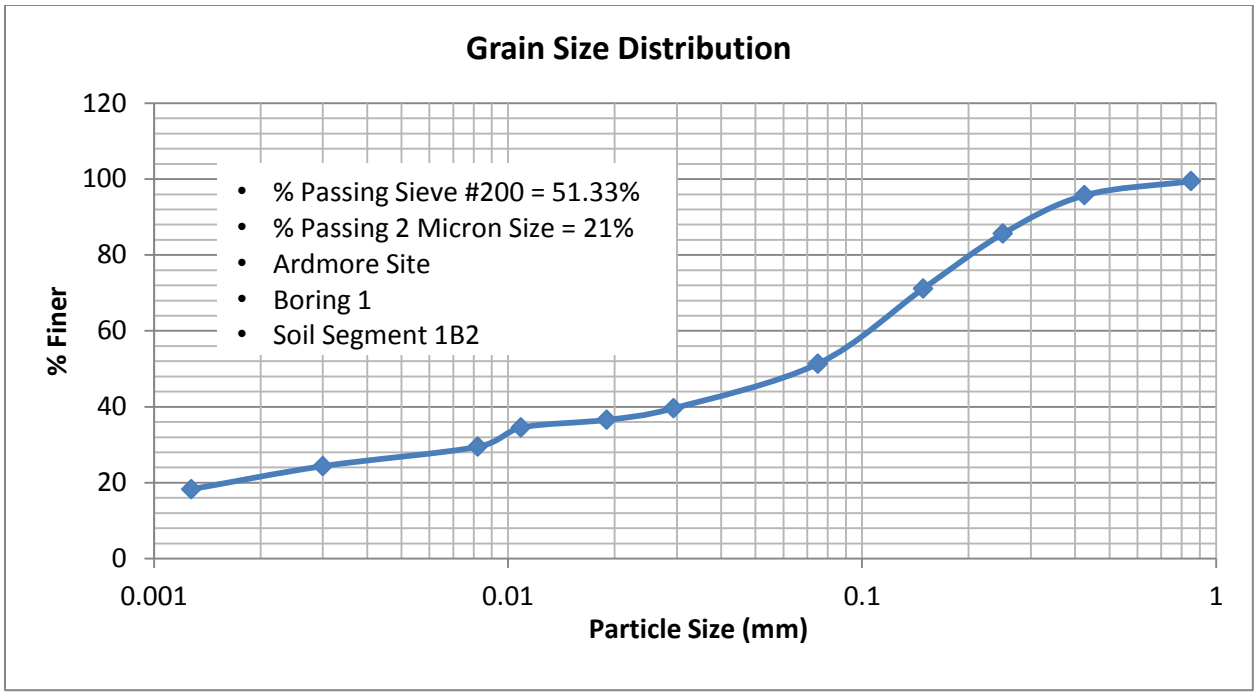

Figure E5. Grain Size Distribution curve for the soil from boring 1, Soil segment 1B2 of Ardmore Site

THIS PAGE IS INTENTIONALLY LEFT BLANK

APPENDIX F

Table F1. Norman Site, Boring 1, Soil Segment 1A3, Depth 1.04 to 1.98 feet

Parameter	Value	Units
Evaporation Coefficient (he)	0.54	cm^{-1}
Atmospheric Suction (Ua)	6.29	pF
Initial Suction (Uo)	3.176	pF
Psychrometer Location (x)	9.2	cm
Sample Length (L)	11.1	cm

Drying Diffusion Coefficient, $\alpha_{dry} = 3.2 \times 10^{-5}$ cm^2/sec (1.92×10^{-3} cm^2/min)

Laboratory Suction Measurements

Time	Suction
(min)	(pF)
2730	3.944
2880	3.988
3030	4.131
3180	4.189
3330	4.252
3480	4.316
3630	4.373
3780	4.415
3930	4.457
4080	4.493

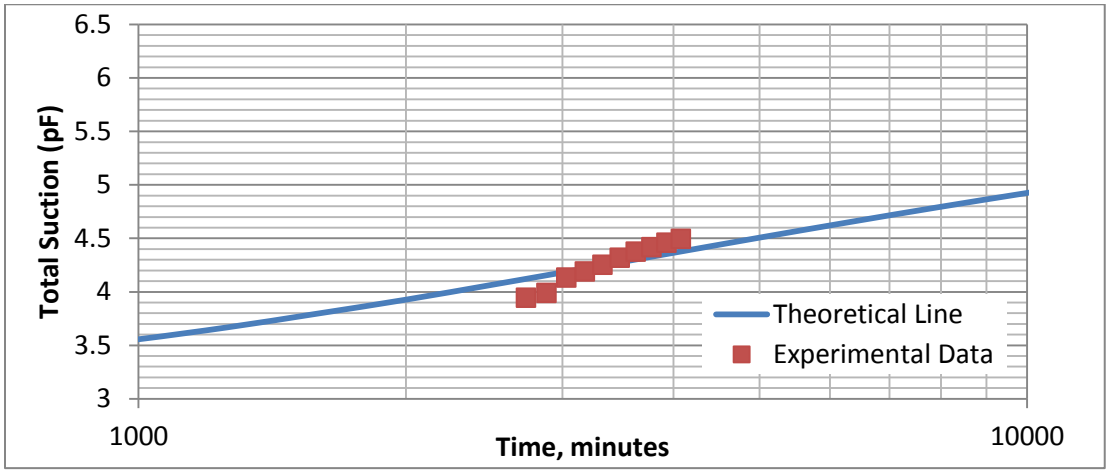

Figure F1. Variation of total suction with time for the soil of Norman site from boring 1, Soil segment 1A3 at a depth of 1.04 to 1.98 feet

Table F2. Norman Site, Boring 2, Soil Segment 2B1, Depth 2.11 to 2.88 feet

Parameter	Value	Units
Evaporation Coefficient (he)	0.54	cm-1
Atmospheric Suction (Ua)	6.292	pF
Initial Suction (Uo)	3.962	pF
Psychrometer Location (x)	18.7	cm
Sample Length (L)	20.7	cm

Drying Diffusion Coefficient, $\alpha_{dry} = 4.33 \times 10^{-6}$ cm^2/sec (2.60×10^{-4} cm^2/min)

Laboratory Suction Measurements

Time	Suction
min	pF
7815	3.964
8185	4.179
8550	4.317
8915	4.426
9285	4.501

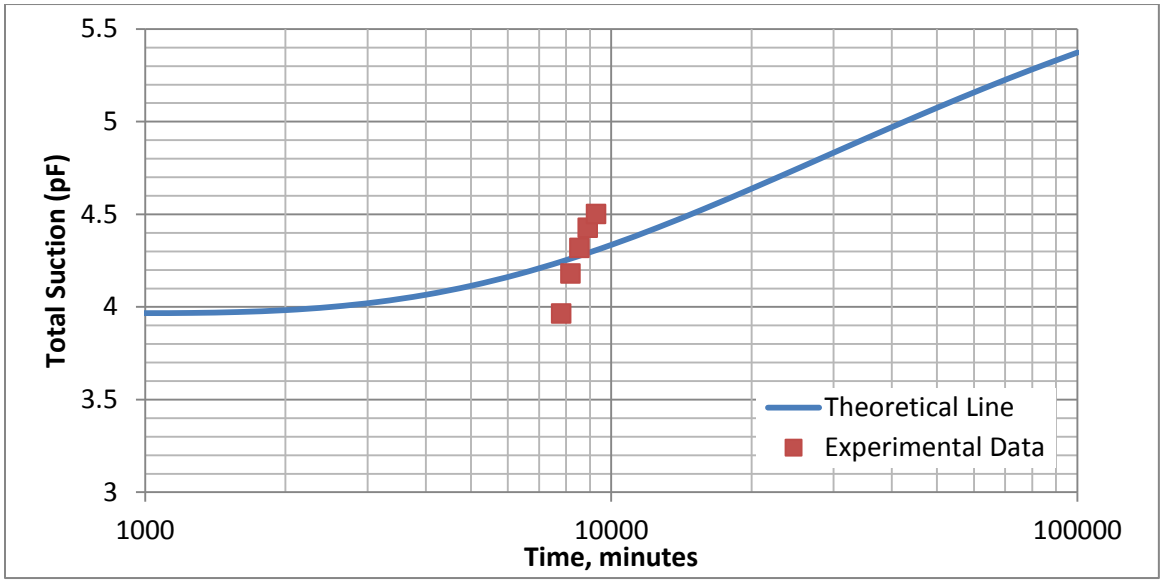

Figure F2. Variation of total suction with time for the soil of Norman site from boring 2, Soil segment 2B1 at a depth of 2.11 to 2.88 feet

Table F3. Norman Site, Boring 2, Soil Segment 2C2, Depth 4.81 to 5.42 feet

Parameter	Value	Units
Evaporation Coefficient (he)	0.54	cm-1
Atmospheric Suction (Ua)	6.140	pF
Initial Suction (Uo)	3.962	pF
Psychrometer Location (x)	5.3	cm
Sample Length (L)	7.0	cm

Drying Diffusion Coefficient, α_{dry} = 1.17 x 10^{-5} cm^2/sec (7.0 x 10^{-4} cm^2/min)

Laboratory Suction Measurements

Time	Suction
min	pF
1805	3.967
1905	4.110
2010	4.217
2115	4.293
2215	4.332

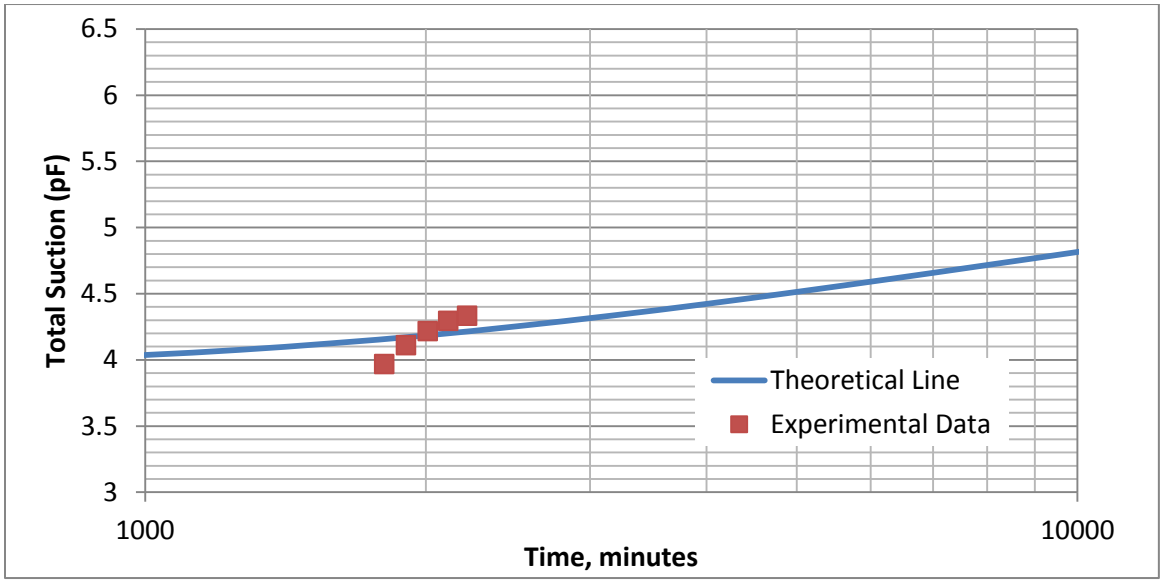

Figure F3. Variation of total suction with time for the soil of Norman site from boring 2, Soil segment 2C2 at a depth of 4.81 to 5.42 feet

Table F4. Norman Site, Boring 2, Soil Segment 2H2, Depth 14.29 to 15.34 feet

Parameter	Value	Units
Evaporation Coefficient (he)	0.54	cm^{-1}
Atmospheric Suction (Ua)	6.279	pF
Initial Suction (Uo)	3.599	pF
Psychrometer Location (x)	16.2	cm
Sample Length (L)	17.2	cm

Drying Diffusion Coefficient, α_{dry} = 2.17 x 10^{-6} cm^2/sec (1.30 x 10^{-4} cm^2/min)

Laboratory Suction Measurements

Time	Suction
min	pF
6250	3.599
6290	3.742
6330	3.830
6380	3.909
6420	3.964
6470	4.040
6520	4.069
6560	4.133
6610	4.169

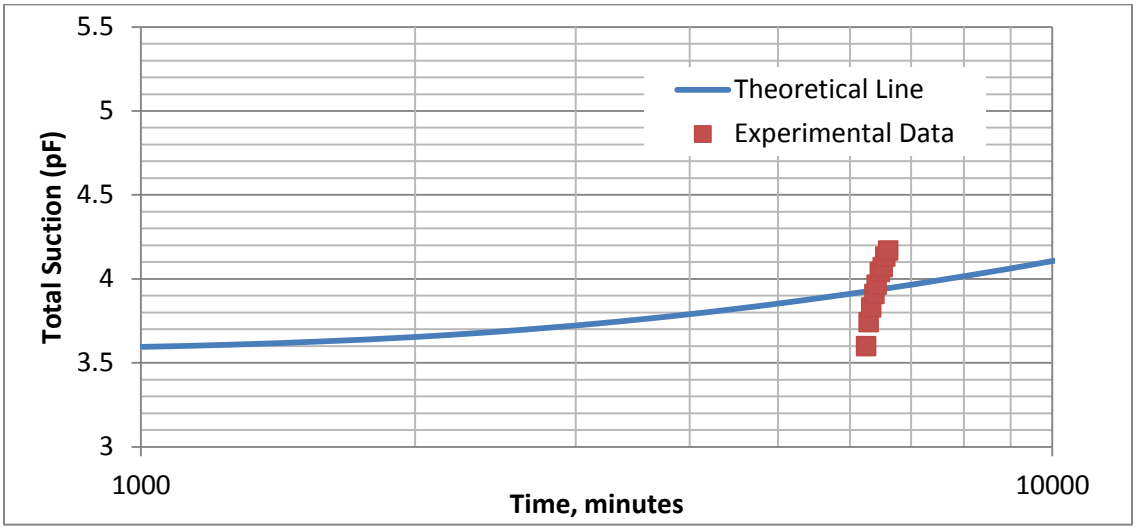

Figure F4. Variation of total suction with time for the soil of Norman site from boring 2, Soil segment 2H2 at a depth of 14.29 to 15.34 feet

Table F5. Norman Site, Boring 3, Soil Segment 3B2, Depth 2.90 to 3.75 feet

Parameter	Value	Units
Evaporation Coefficient (he)	0.54	cm^{-1}
Atmospheric Suction (Ua)	6.275	pF
Initial Suction (Uo)	3.809	pF
Psychrometer Location (x)	17.6	cm
Sample Length (L)	19.1	cm

Drying Diffusion Coefficient, $\alpha_{dry} = 1.72 \times 10^{-5}$ cm^2/sec (1.03×10^{-3} cm^2/min)

Laboratory Suction Measurements

Time	Suction
min	pF
715	3.809
1065	4.024
1415	4.172
1765	4.261
2125	4.326
2475	4.382
2825	4.433
3175	4.463
3525	4.490

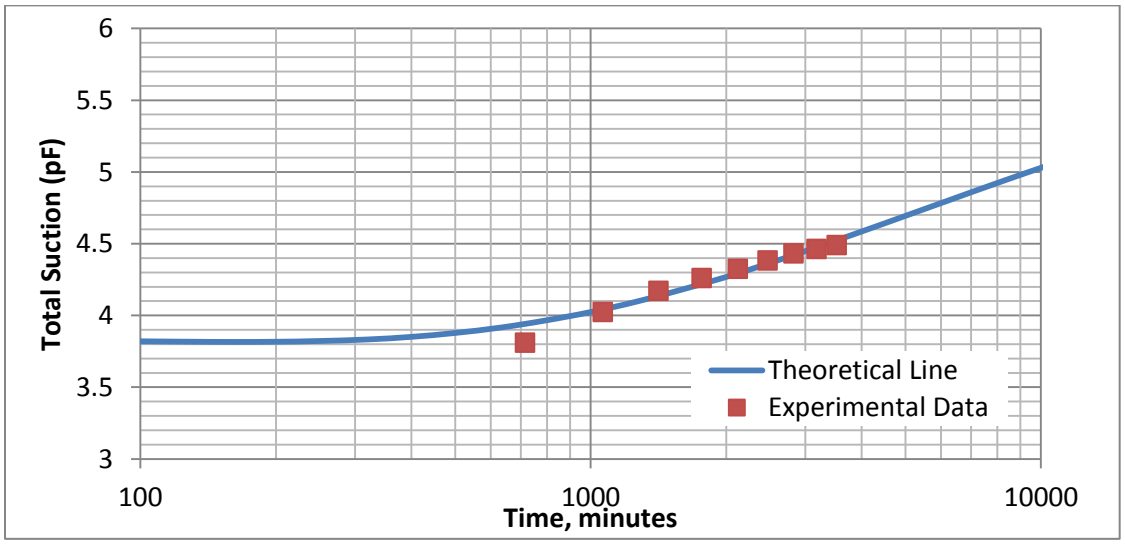

Figure F5. Variation of total suction with time for the soil of Norman site from boring 3, Soil segment 3B2 at a depth of 2.90 to 3.75 feet

Table F6. Norman Site, Boring 3, Soil Segment 3C2, Depth 4.83 to 5.90 feet

Parameter	Value	Units
Evaporation Coefficient (he)	0.54	cm^{-1}
Atmospheric Suction (Ua)	6.272	pF
Initial Suction (Uo)	3.582	pF
Psychrometer Location (x)	26.0	cm
Sample Length (L)	29.0	cm

Drying Diffusion Coefficient, $\alpha_{dry} = 9.0 \times 10^{-5}$ cm^2/sec (5.40×10^{-3} cm^2/min)

Laboratory Suction Measurements

Time	Suction
min	pF
510	3.582
780	4.061
1050	4.244
1320	4.352
1590	4.415
1850	4.459
2120	4.489
2390	4.514
2660	4.524
2930	4.527

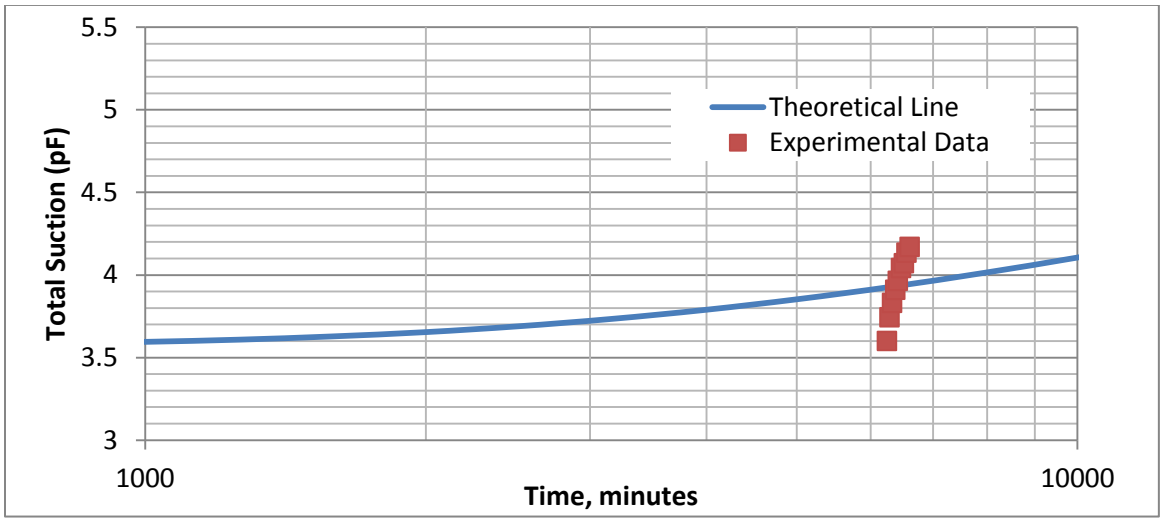

Figure F6. Variation of total suction with time for the soil of Norman site from boring 3, Soil segment 3C2 at a depth of 4.83 to 5.90 feet

Table F7. Norman Site, Boring 4, Soil Segment 4A1, Depth 0 to 0.87 feet

Parameter	Value	Units
Evaporation Coefficient (he)	0.54	cm^{-1}
Atmospheric Suction (Ua)	6.31	pF
Initial Suction (Uo)	3.61	pF
Psychrometer Location (x)	22.9	cm
Sample Length (L)	24.9	cm

Drying Diffusion Coefficient, $\alpha_{dry} = 1.68 \times 10^{-5}$ cm^2/sec (1.01×10^{-3} cm^2/min)

Laboratory Suction Measurements

Time	Suction
min	pF
2950	3.61
3230	3.85
3520	4.04
3810	4.21
4090	4.34
4380	4.43
4670	4.50
4950	4.57
5240	4.61

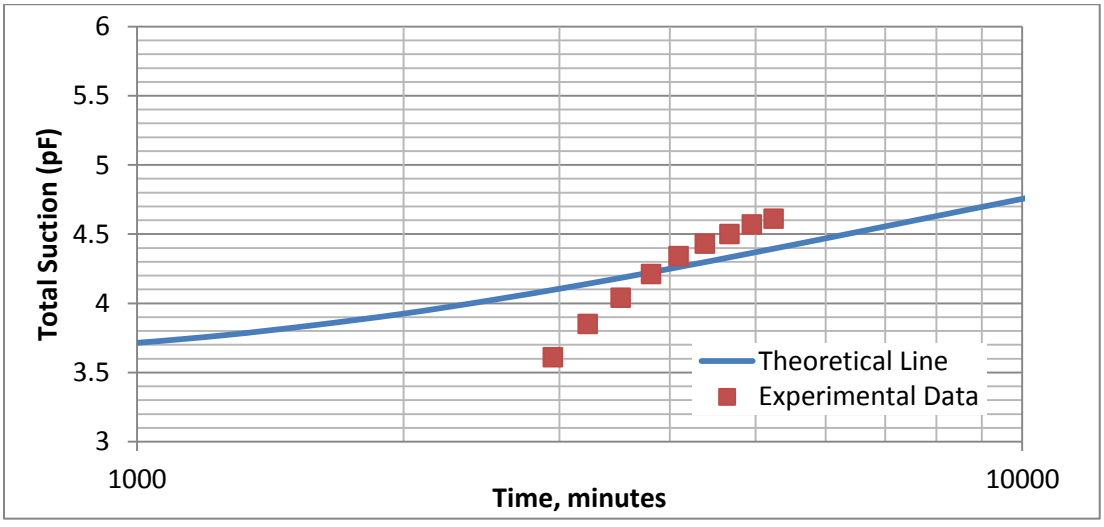

Figure F7. Variation of total suction with time for the soil of Norman site from boring 4, Soil segment 4A1 at a depth of 0 to 0.87 feet

Table F8. Norman Site, Soil Segment 4D2, Depth 7.40 to 8.0 feet

Parameter	Value	Units
Evaporation Coefficient (he)	0.54	cm^{-1}
Atmospheric Suction (Ua)	6.29	pF
Initial Suction (Uo)	3.69	pF
Psychrometer Location (x)	14.9	cm
Sample Length (L)	17.9	cm

Drying Diffusion Coefficient, $\alpha_{dry} = 4.33 \times 10^{-5}$ cm^2/sec (2.60×10^{-3} cm^2/min)

Laboratory Suction Measurements

Time	Suction
min	pF
1540	3.75
1810	4.02
2080	4.19
2350	4.27
2630	4.35
2900	4.40
3170	4.45
3440	4.49
3710	4.51

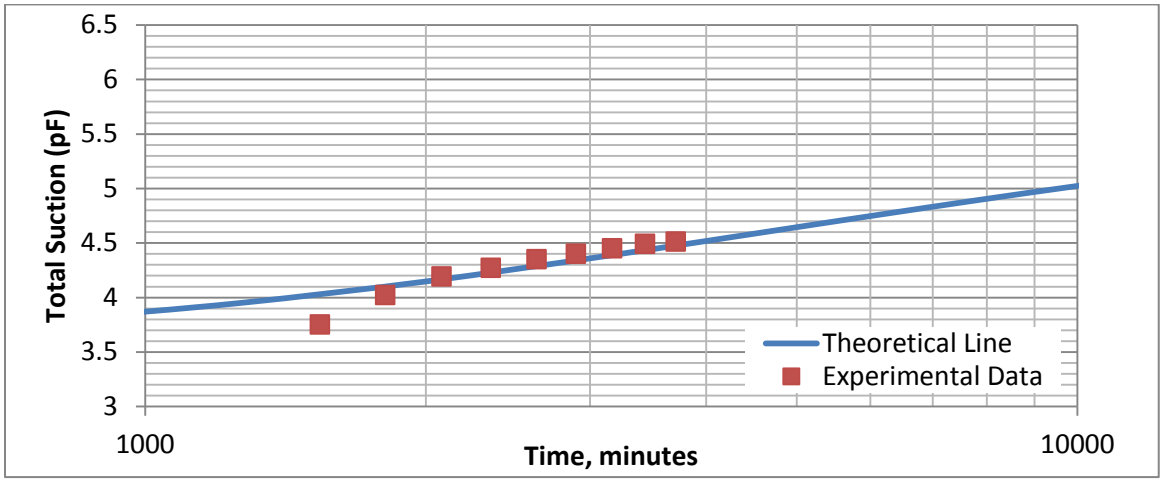

Figure F8. Variation of total suction with time for the soil of Norman site from boring 4, Soil segment 4D2 at a depth of 7.40 to 8.0 feet

Table F9. Norman Site, Compacted Sample, Soil Segments 2F1, 2F2, 2H2, Soil Type 2

Parameter	Value	Units
Evaporation Coefficient, h_e	0.54	cm^{-1}
Atmospheric Suction, U_a	6.29	pF
Initial Suction, U_o	3.59	pF
Psychrometer Location, X	14.3	cm
Sample Length, L	16.8	cm

Drying Diffusion Coefficient, $\alpha_{dry} = 8.0 \times 10^{-5}$ cm^2/sec (4.80×10^{-3} cm^2/min)

Laboratory Suction Measurements

Time	Suction
min	pF
470	3.59
500	3.68
550	3.80
600	3.91
680	4.02
770	4.13
920	4.24
1150	4.35
1500	4.46
2640	4.56

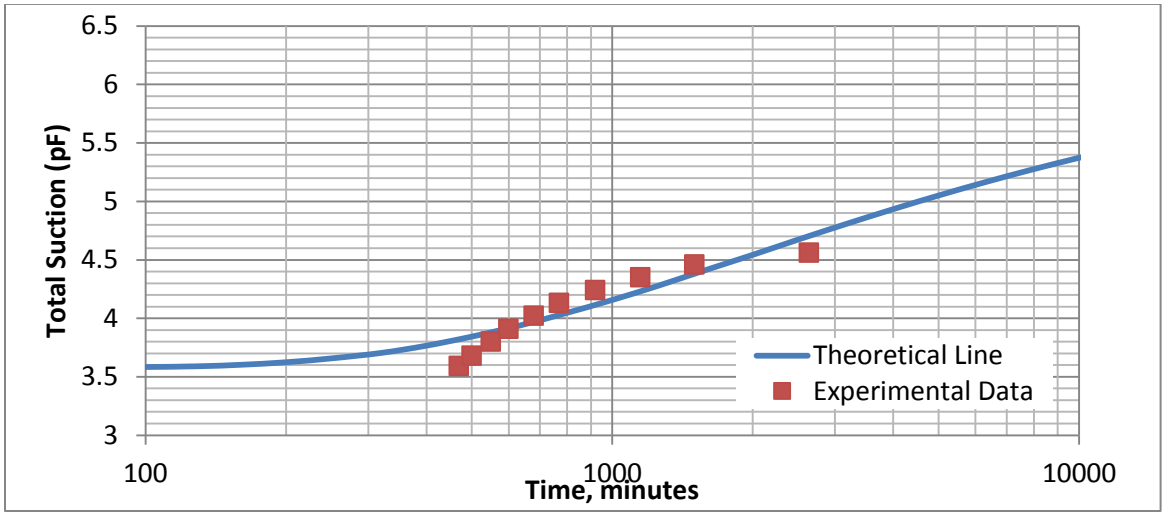

Figure F9. Variation of total suction with time for compacted samples of Norman site soil from the segments 2F1, 2F2, 2H2 of soil type 2

Table F10. Norman Site, Compacted Sample, Soil Segments 1A1, 2A1, Soil Type 1

Parameter	Value	Units
Evaporation Coefficient, h_e	0.54	cm^{-1}
Atmospheric Suction, U_a	6.21	pF
Initial Suction, U_o	3.38	pF
Psychrometer Location, X	14.6	cm
Sample Length, L	16.6	cm

Drying Diffusion Coefficient, $\alpha_{dry} = 4.45 \times 10^{-5}$ cm^2/sec (2.67×10^{-3} cm^2/min)

Laboratory Suction Measurements

Time	Suction
Min	pF
10	4.38
450	4.40
1200	4.42
1950	4.44
2600	4.45
3450	4.47
4760	4.50
4820	4.50
6230	4.53
6930	4.54

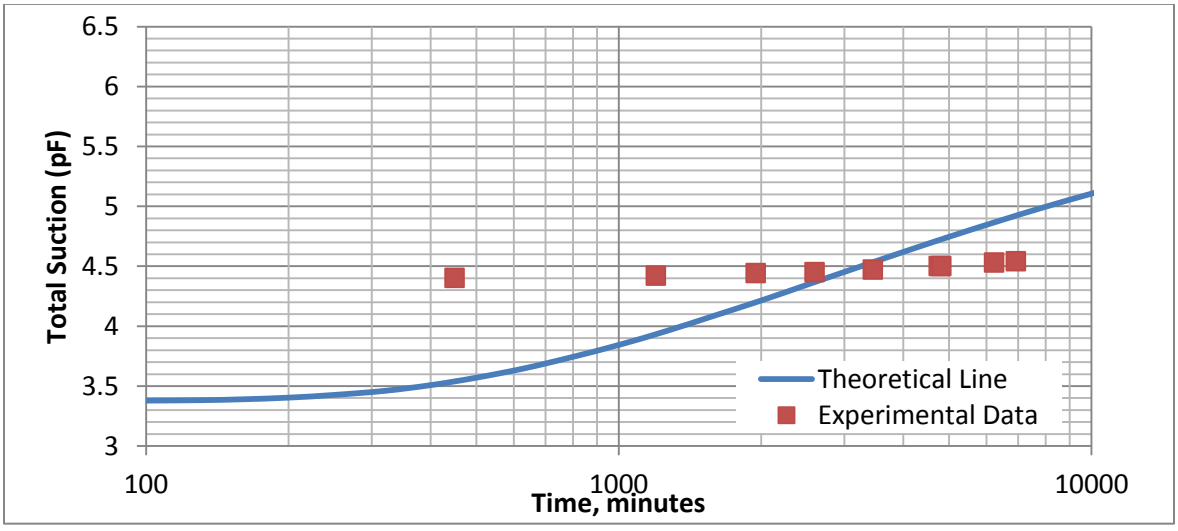

Figure F10. Variation of total suction with time for compacted samples of Norman site soil from the segments 1A1, 2A1 of soil type 1

APPENDIX G

Table G1. Lake Hefner Site, Boring 1, Soil Segment 1A1, Depth 0 to 0.80 Feet

Parameter	Value	Unit
Evaporation Coefficient, h_e	0.54	cm^{-1}
Atmospheric Suction, U_a	6.30	pF
Initial Suction, U_o	3.01	pF
Psychrometer Location, X	21.5	cm
Sample Length, L	23	cm

Drying Diffusion Coefficient, $\alpha_{dry} = 6.67 \times 10^{-5}$ cm^2/sec (4.00×10^{-3} cm^2/min)

Laboratory Suction Measurements

Time	Suction
min	pF
1020	3.71
1060	3.86
1110	3.98
1160	4.08
1200	4.15
1250	4.21
1300	4.32
1340	4.37
1390	4.39

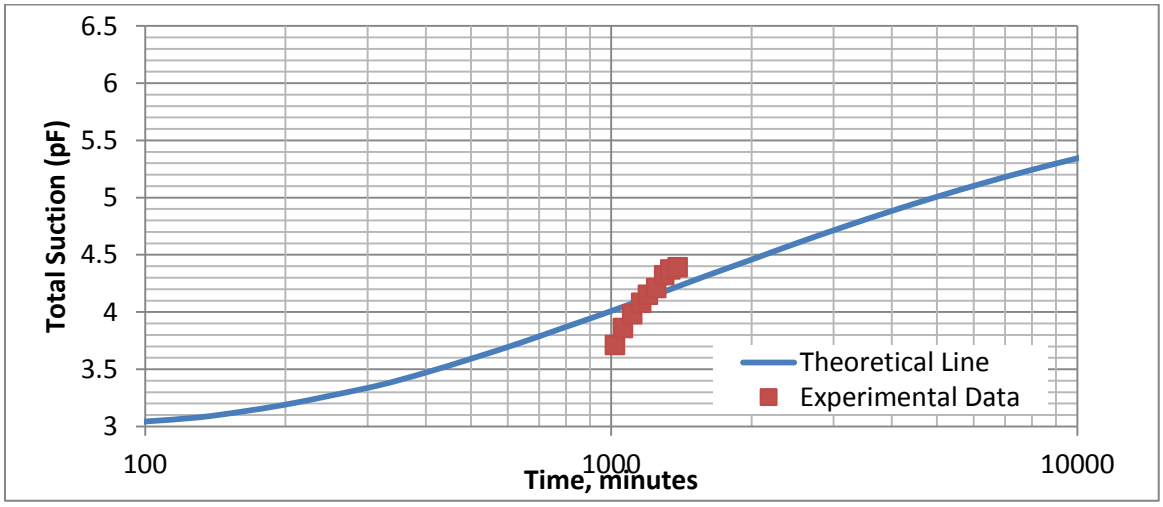

Figure G1. Variation of total suction with time for the soil of Lakehefner Site from boring 1, Soil segment 1A1 at a depth of 0 to 0.80 Feet

Table G2. Lake Hefner Site, Boring 2, Soil Segment 2C1, Depth 4 to 4.87 Feet

Parameter	Value	Unit
Evaporation Coefficient, h_e	0.54	cm^{-1}
Atmospheric Suction, U_a	6.29	pF
Initial Suction, U_o	3.66	pF
Psychrometer Location, X	19.7	cm
Sample Length, L	22.7	cm

Drying Diffusion Coefficient, α_{dry} = 8.83 x 10^{-5} cm^2/sec (5.30 x 10^{-3} cm^2/min)

Laboratory Suction Measurements

Time	Suction
min	pF
700	3.66
820	3.90
930	4.07
1040	4.17
1160	4.28
1270	4.33
1380	4.39
1500	4.43
1610	4.45

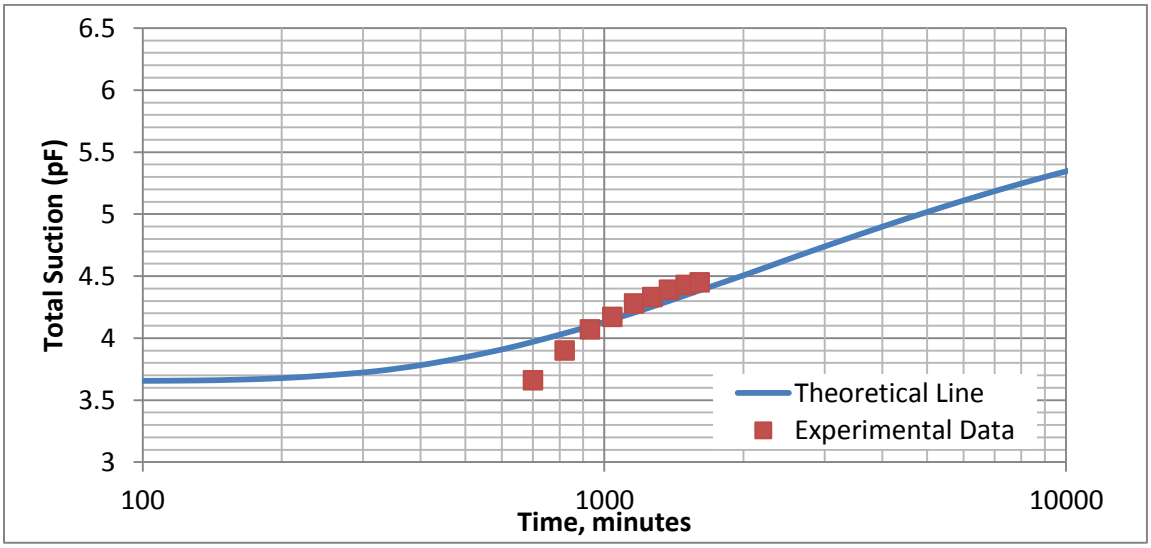

Figure G2. Variation of total suction with time for the soil of Lakehefner Site from boring 2, Soil segment 2C1 at a depth of 4 to 4.87 Feet

Table G3. Lake Hefner Site, Boring 2, Soil Segment 2D2, Depth 6.98 to 7.96 Feet

Parameter	Value	Unit
Evaporation Coefficient, h_e	0.54	cm^{-1}
Atmospheric Suction, U_a	6.30	pF
Initial Suction, U_o	3.30	pF
Psychrometer Location, X	12	cm
Sample Length, L	15	cm

Drying Diffusion Coefficient, $\alpha_{dry} = 8.92 \times 10^{-5}$ cm^2/sec (5.35×10^{-3} cm^2/min)

Laboratory Suction Measurements

Time	Suction
min	pF
1400	3.84
1680	4.07
1960	4.22
2240	4.32
2530	4.40
2810	4.47
3090	4.53
3370	4.57
3650	4.59

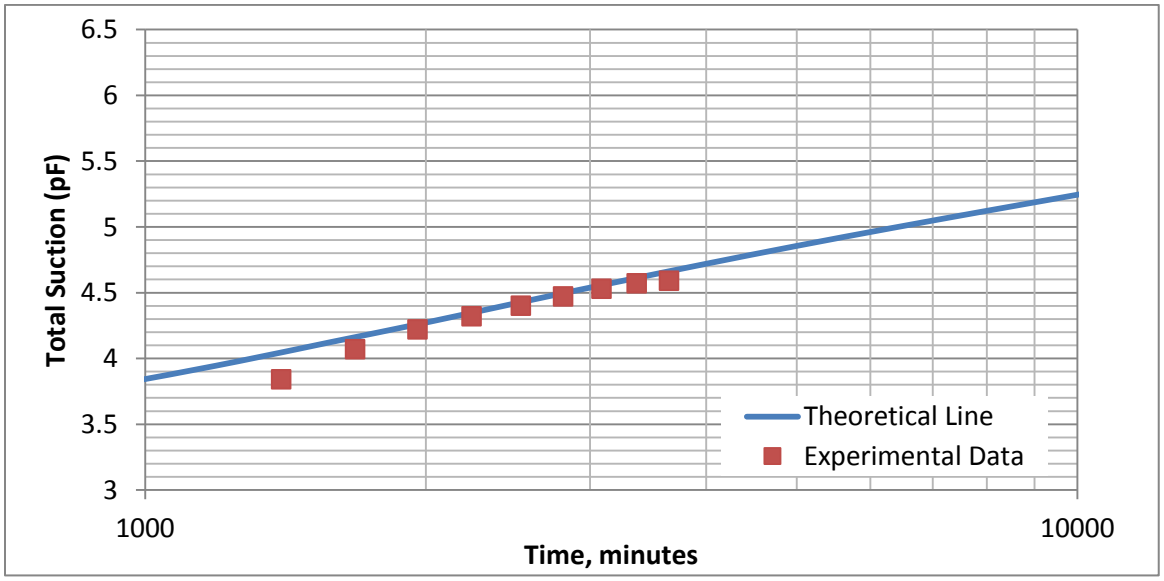

Figure G3. Variation of total suction with time for the soil of Lakehefner site from boring 2, Soil segment 2D2 at a depth of 6.98 to 7.96 feet

Table G4. Lake Hefner Site, Boring 3, Soil Segment 3A2, Depth 0.80 to 1.5 Feet

Parameter	Value	Unit
Evaporation Coefficient, h_e	0.54	cm^{-1}
Atmospheric Suction, U_a	6.27	pF
Initial Suction, U_o	3.29	pF
Psychrometer Location, X	12.3	cm
Sample Length, L	14.8	cm

Drying Diffusion Coefficient, α_{dry} = 3.67 x 10^{-5} cm^2/sec (2.20 x 10^{-3} cm^2/min)

Laboratory Suction Measurements

Time	Suction
min	pF
1960	3.65
2300	3.91
2630	4.06
2970	4.16
3300	4.22
3640	4.29
3970	4.33
4310	4.35
4640	4.37

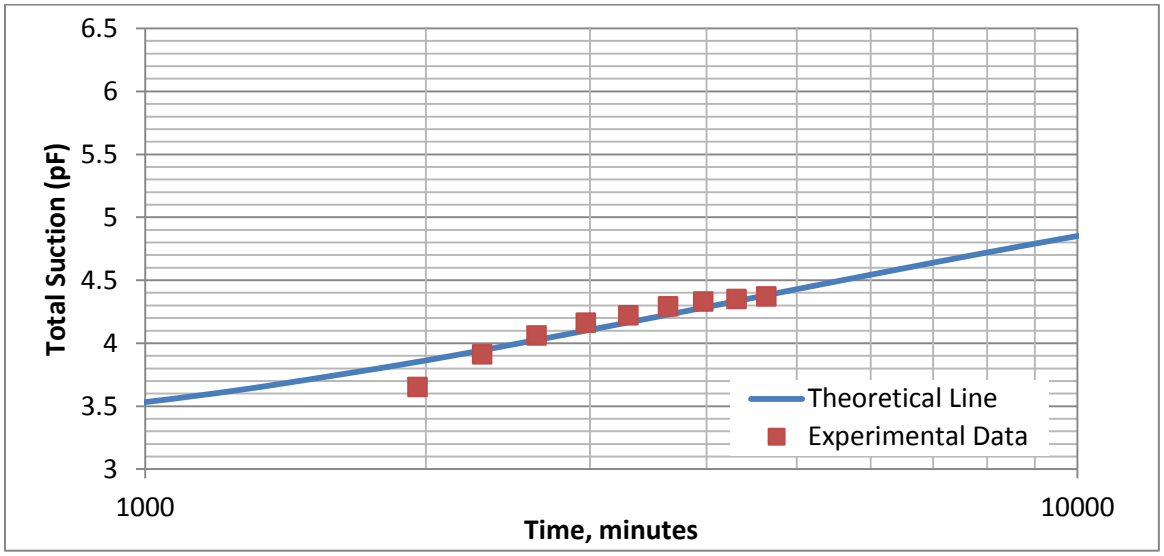

Figure G4. Variation of total suction with time for the soil of Lakehefner site from boring 3, Soil segment 3A2 at a depth of 0.80 to 1.5 feet

Table G5. Lake Hefner Site, Boring 3, Soil Segment 3C2, Depth 4.50 to 5.45 Feet

Parameter	Value	Unit
Evaporation Coefficient, h_e	0.54	cm^{-1}
Atmospheric Suction, U_a	6.32	pF
Initial Suction, U_o	3.74	pF
Psychrometer Location, X	16	cm
Sample Length, L	18	cm

Drying Diffusion Coefficient, $\alpha_{dry} = 5.33 \times 10^{-5}$ cm^2/sec (3.20×10^{-3} cm^2/min)

Laboratory Suction Measurements

Time	Suction
min	pF
510	3.74
580	3.90
660	4.02
740	4.12
810	4.20
890	4.27
970	4.33
1040	4.37
1120	4.39

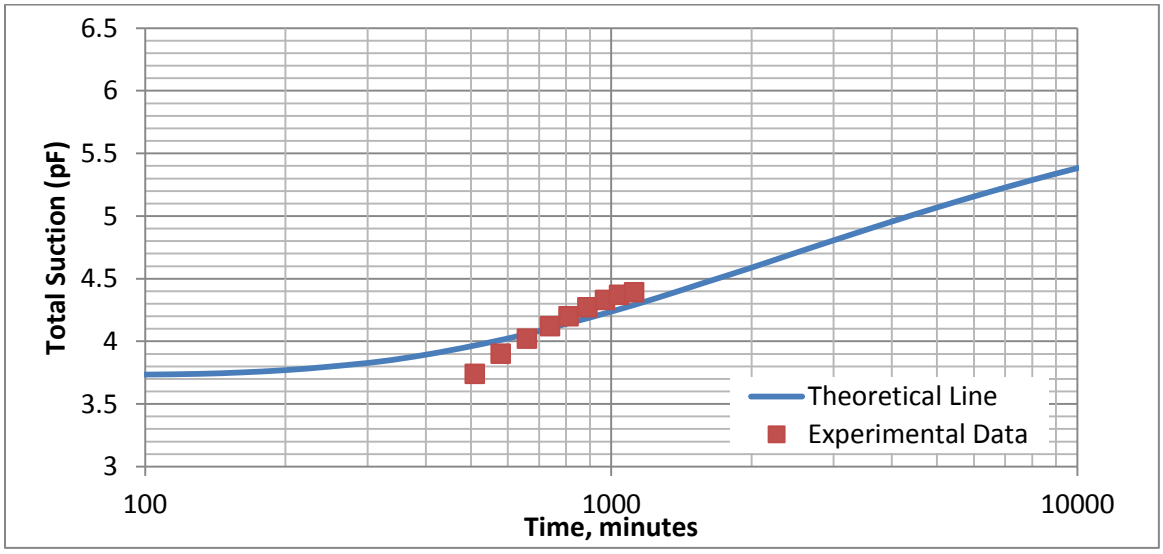

Figure G5 Variation of total suction with time for the soil of Lakehefner site from boring 3, Soil segment 3C2 at a depth of 4.50 to 5.45 feet

Table G6. Lake Hefner Site, Compacted Sample, Soil Segments 1C2, 2C3, 2D1, Soil Type 2

Parameter	Value	Unit
Evaporation Coefficient, h_e	0.54	cm^{-1}
Atmospheric Suction, U_a	6.19	pF
Initial Suction, U_o	3.53	pF
Psychrometer Location, x	1.5	cm
Sample Length, L	16.7	cm

Drying Diffusion Coefficient, $\alpha_{dry} = 4.66 \times 10^{-6}$ cm^2/sec (2.80×10^{-4} cm^2/min)

Laboratory Suction Measurements

Time	Suction
min	pF
4150	3.53
4240	3.61
4280	3.66
4400	3.75
4460	3.79
4530	3.88
4600	3.93
4670	3.97
4930	4.07
5200	4.13

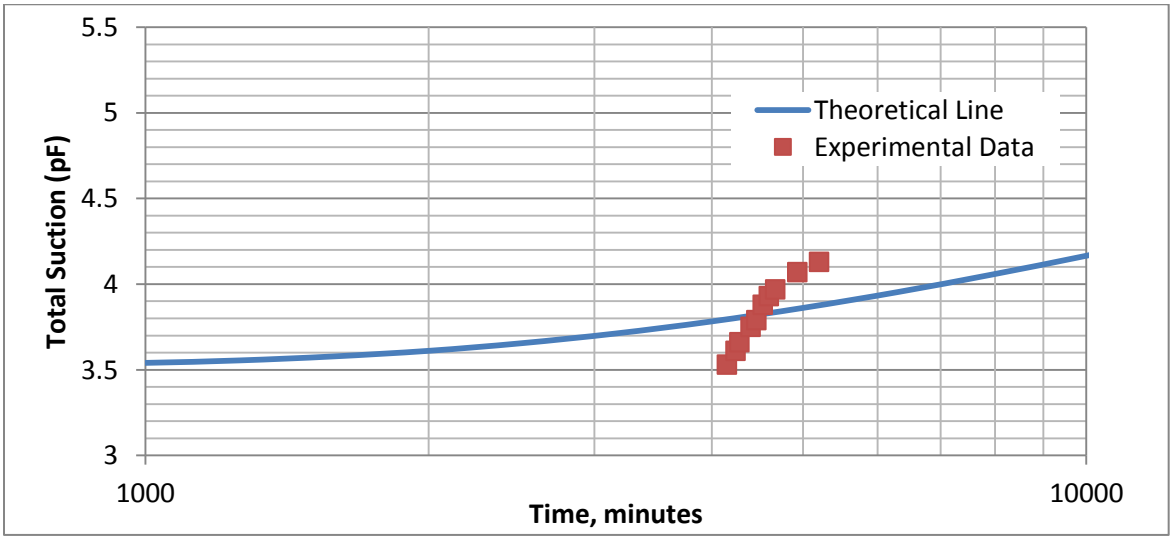

Figure G6. Variation of total suction with time for compacted samples of Lakehefner Site soil from the segments 1C2, 2C3, 2D1 of soil type 2

APPENDIX H

Table H1. Ardmore Site, Boring 1, Soil Segment 1B1, Depth 2.0 to 2.80 Feet

Parameter	Value	Unit
Evaporation Coefficient, h_e	0.54	cm^{-1}
Atmospheric Suction, U_a	6.25	pF
Initial Suction, U_o	3.42	pF
Psychrometer Location, x	15.5	cm
Sample Length, L	17.5	cm

Drying Diffusion Coefficient, $\alpha_{dry} = 3.30 \times 10^{-5}$ cm^2/sec (1.98×10^{-3} cm^2/min)

Laboratory Suction Measurements

Time	Suction
min	pF
1640	3.42
1700	3.70
1760	3.88
1820	4.00
1880	4.11
1950	4.19
2010	4.25
2070	4.30
2130	4.33
2190	4.35

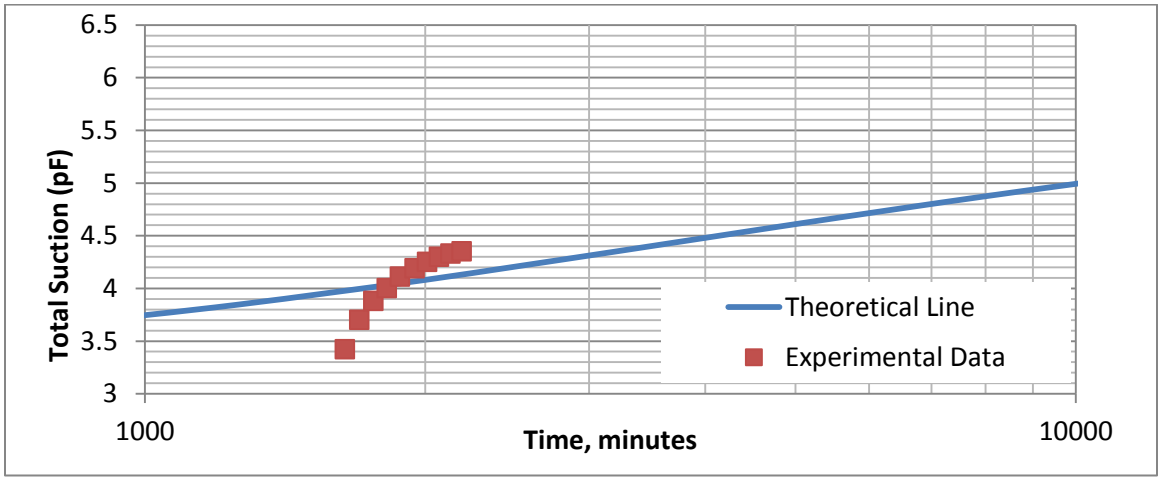

Figure H1. Variation of total suction with time for the soil of Ardmore site from Boring 1, Soil segment 1B1 at a Depth of 2.0 to 2.80 feet

Table H2. Ardmore Site, Boring 3, Soil Segment 3C2, Depth 4.90 to 6.0 Feet

Parameter	Value	Unit
Evaporation Coefficient, h_e	0.54	cm^{-1}
Atmospheric Suction, U_a	6.22	pF
Initial Suction, U_o	3.37	pF
Psychrometer Location, x	26.1	cm
Sample Length, L	28.6	cm

Drying Diffusion Coefficient, $\alpha_{dry} = 1.02 \times 10^{-4}$ cm^2/sec (6.11×10^{-3} cm^2/min)

Laboratory Suction Measurements

Time	Suction
min	pF
450	3.37
480	3.50
520	3.64
580	3.78
660	3.90
760	4.04
910	4.17
1100	4.30
1440	4.44
2010	4.57

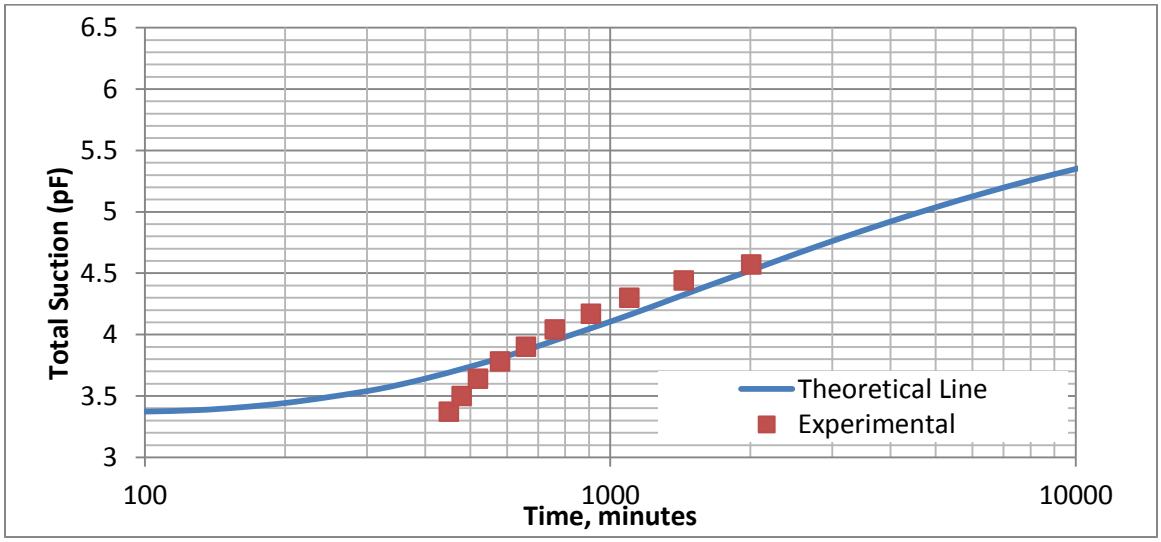

Figure H2. Variation of total suction with time for the soil of Ardmore site from boring 3, Soil segment 3C2 at a depth of 4.90 to 6.0 feet

Table H3. Ardmore Site, Boring 4, Soil Segment 1BB2, Depth 2.50 to 3.40 Feet

Parameter	Value	Unit
Evaporation Coefficient, h_e	0.54	cm^{-1}
Atmospheric Suction, U_a	6.29	pF
Initial Suction, U_o	3.91	pF
Psychrometer Location, x	20.2	cm
Sample Length, L	23.2	cm

Drying Diffusion Coefficient, $\alpha_{dry} = 7.08 \times 10^{-5}$ cm^2/sec (4.25×10^{-3} cm^2/min)

Laboratory Suction Measurements

Time	Suction
min	pF
100	3.91
220	3.99
330	4.06
490	4.14
710	4.22
1000	4.29
1290	4.37
1630	4.44
2000	4.52
2560	4.60

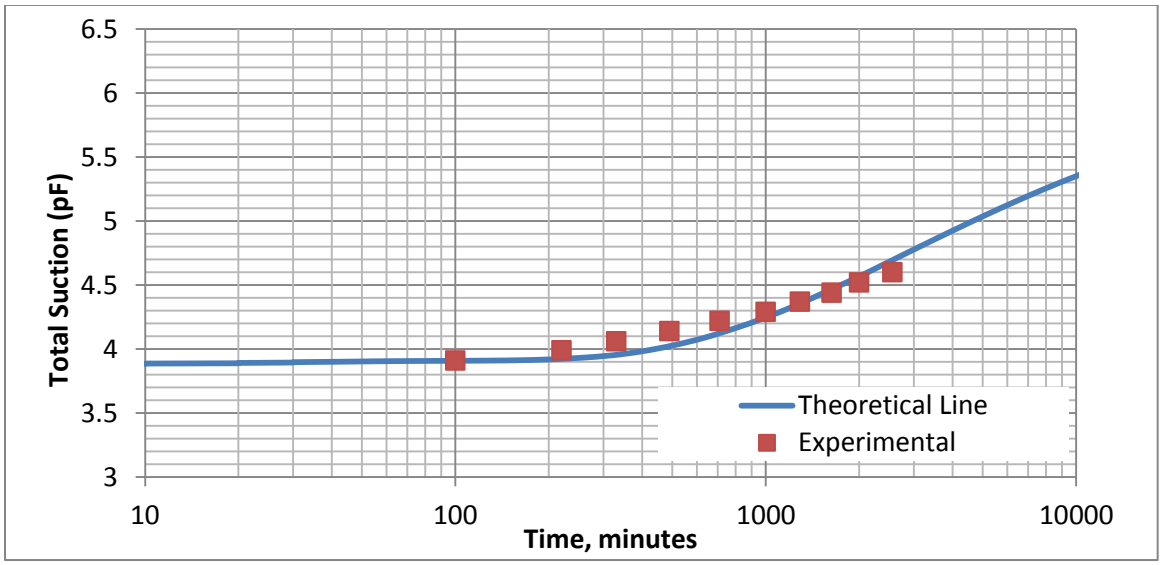

Figure H3. Variation of total suction with time for the soil of Ardmore site from boring 4, Soil segment 1BB2 at a depth of 2.50 to 3.40 feet

Table H4. Ardmore Site, Boring 4, Soil Segment 1CC1, Depth 4.0 to 4.88 Feet

Parameter	Value	Unit
Evaporation Coefficient, h_e	0.54	cm^{-1}
Atmospheric Suction, U_a	6.29	pF
Initial Suction, U_o	3.0	pF
Psychrometer Location, x	17.5	cm
Sample Length, L	21.0	cm

Drying Diffusion Coefficient, $\alpha_{dry} = 1.55 \times 10^{-4}$ cm^2/sec (9.30×10^{-3} cm^2/min)

Laboratory Suction Measurements

Time	Suction
min	pF
460	3.13
510	3.30
570	3.47
660	3.63
820	3.80
1060	3.96
1410	4.11
1980	4.28
2660	4.44
3860	4.61

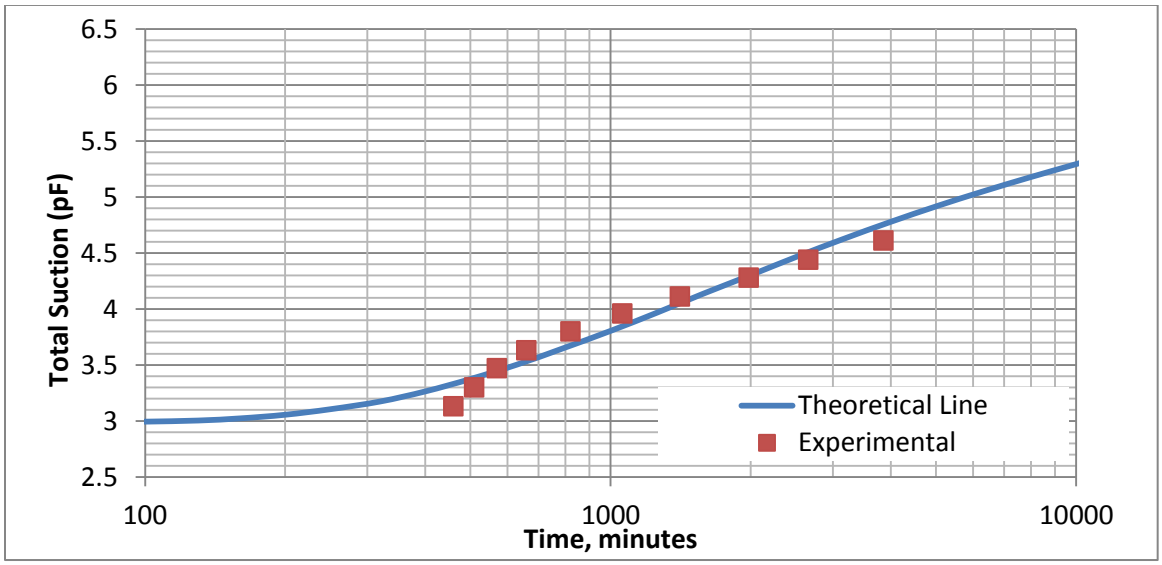

Figure H4. Variation of total suction with time for the soil of Ardmore site from boring 4, Soil segment 1CC1 at a depth of 4.0 to 4.88 feet

Table H5. Ardmore Site, Boring 5, Soil Segment 2BB2, Depth 2.90 to 4.0 Feet

Parameter	Value	Unit
Evaporation Coefficient, h_e	0.54	cm^{-1}
Atmospheric Suction, U_a	6.21	pF
Initial Suction, U_o	3.54	pF
Psychrometer Location, x	16.5	cm
Sample Length, L	18.0	cm

Drying Diffusion Coefficient, $\alpha_{dry} = 1.08 \times 10^{-5}$ cm^2/sec (6.50×10^{-4} cm^2/min)

Laboratory Suction Measurements

Time	Suction
min	pF
2740	3.54
2790	3.65
2840	3.75
2910	3.86
3000	3.97
3130	4.09
3280	4.18
3500	4.29
3810	4.40
4420	4.51

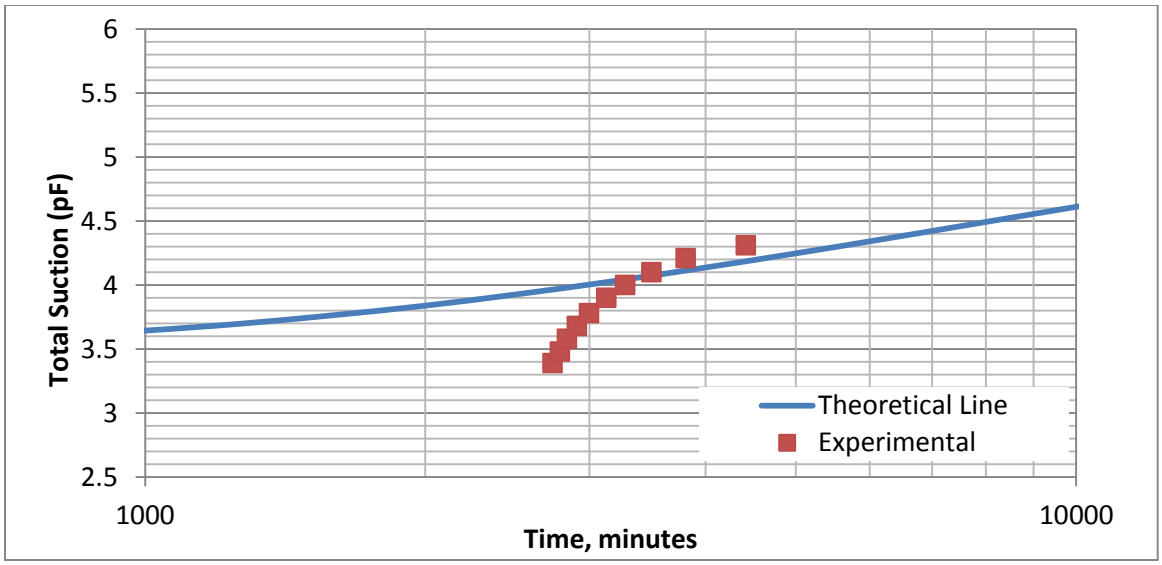

Figure H5. Variation of total suction with time for the soil of Ardmore site from boring 5, Soil segment 2BB2 at a depth of 2.90 to 4.0 feet

Table H6. Ardmore Site, Boring 5, Soil Segment 2CC2, Depth 4.86 to 5.86 Feet

Parameter	Value	Unit
Evaporation Coefficient, h_e	0.54	cm^{-1}
Atmospheric Suction, U_a	6.13	pF
Initial Suction, U_o	3.39	pF
Psychrometer Location, x	19.6	cm
Sample Length, L	21.6	cm

Drying Diffusion Coefficient, $\alpha_{dry} = 1.30 \times 10^{-5}$ cm^2/sec (7.80×10^{-4} cm^2/min)

Laboratory Suction Measurements

Time	Suction
min	pF
3190	3.39
3210	3.48
3300	3.58
3350	3.68
3460	3.78
3590	3.90
3730	4.00
3880	4.10
4100	4.21
4570	4.31

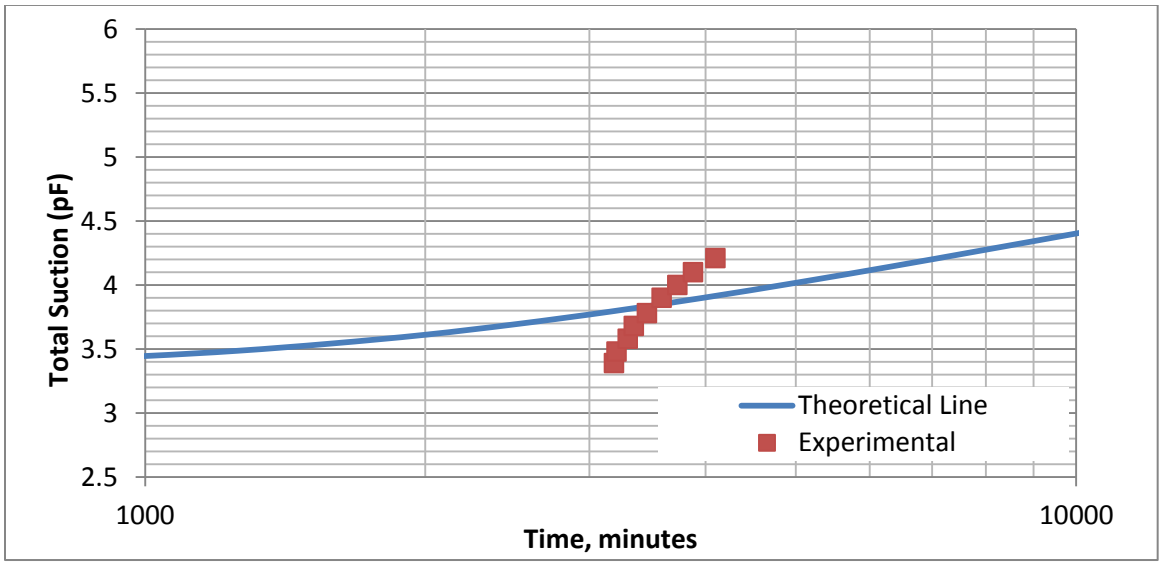

Figure H6. Variation of total suction with time for the soil of Ardmore site from boring 5, Soil segment 2CC2 at a depth of 4.86 to 5.86 feet

Table H7. Ardmore Site, Boring 6, Soil Segment 3AA2, Depth 0.1 to 1.1 Feet

Parameter	Value	Unit
Evaporation Coefficient, h_e	0.54	cm^{-1}
Atmospheric Suction, U_a	6.19	pF
Initial Suction, U_o	3.52	pF
Psychrometer Location, x	21.0	cm
Sample Length, L	23.0	cm

Drying Diffusion Coefficient, $\alpha_{dry} = 3.43 \times 10^{-5}$ cm^2/sec (2.06×10^{-3} cm^2/min)

Laboratory Suction Measurements

Time	Suction
min	pF
990	3.52
1020	3.61
1090	3.70
1210	3.85
1360	3.97
1540	4.08
1800	4.21
2110	4.32
2550	4.44
3400	4.59

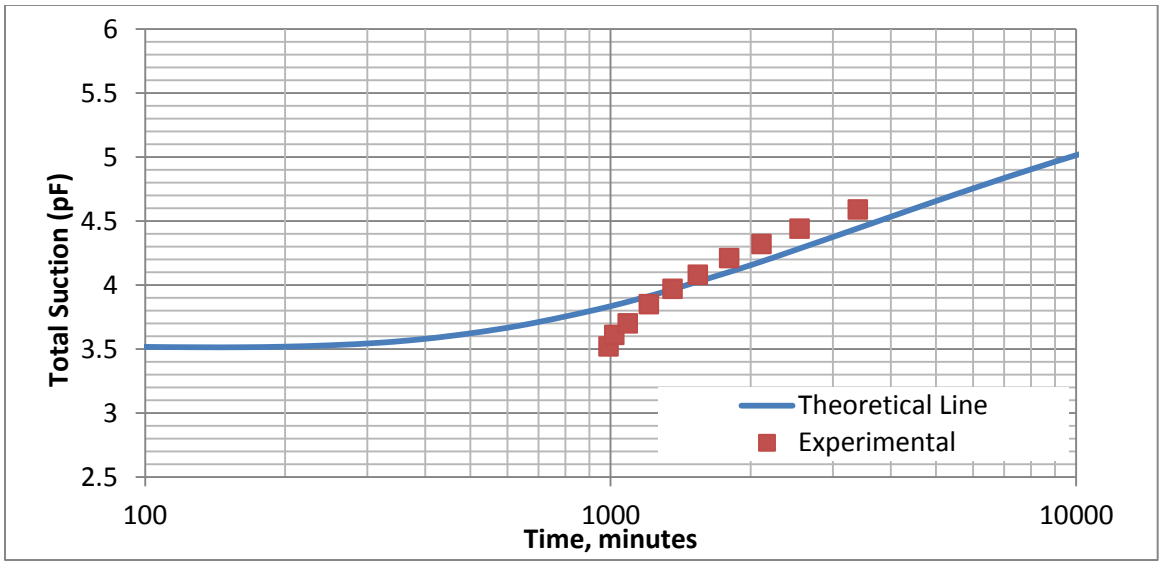

Figure H7. Variation of total suction with time for the soil of Ardmore site from boring 6, Soil segment 3AA2 at a depth of 0.1 to 1.1 feet

Table H8. Ardmore Site, Boring 6, Soil Segment 3DD1, Depth 6.0 to 6.5 Feet

Parameter	Value	Unit
Evaporation Coefficient, h_e	0.54	cm^{-1}
Atmospheric Suction, U_a	6.21	pF
Initial Suction, U_o	3.51	pF
Psychrometer Location, x	12.4	cm
Sample Length, L	14.9	cm

Drying Diffusion Coefficient, $\alpha_{dry} = 1.62 \times 10^{-5}$ cm^2/sec (9.7×10^{-4} cm^2/min)

Laboratory Suction Measurements

Time	Suction
min	pF
3590	3.51
3690	3.63
3800	3.73
3950	3.85
4150	3.96
4360	4.07
4640	4.18
4980	4.29
5430	4.40
6070	4.52

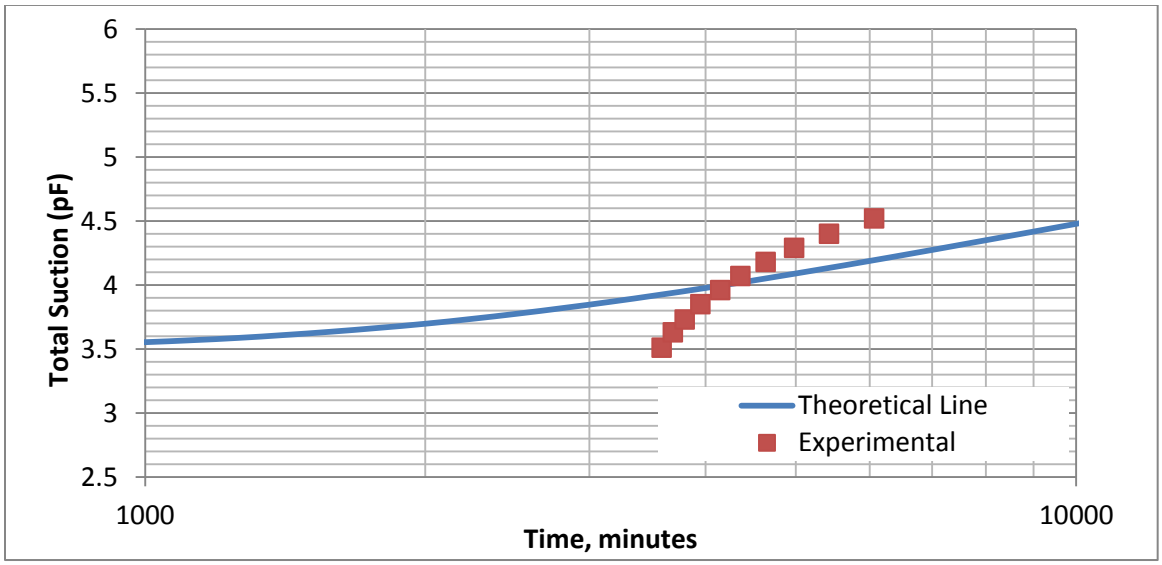

Figure H8. Variation of total suction with time for the soil of Ardmore site from boring 6, Soil segment 3DD1 at a depth of 6.0 to 6.5 feet

Table H9. Ardmore Site, Boring 7, Soil Segment 4AA2, Depth 0.95 to 2.0 Feet

Parameter	Value	Unit
Evaporation Coefficient, h_e	0.54	cm^{-1}
Atmospheric Suction, U_a	6.08	pF
Initial Suction, U_o	3.68	pF
Psychrometer Location, x	15	cm
Sample Length, L	17.5	cm

Drying Diffusion Coefficient, $\alpha_{dry} = 9.0 \times 10^{-6}$ cm^2/sec (5.4×10^{-4} cm^2/min)

Laboratory Suction Measurements

Time	Suction
min	pF
6140	3.68
6410	3.78
6700	3.89
7030	3.98
7500	4.09
8080	4.19
8660	4.29
9510	4.39
10660	4.50
12600	4.61

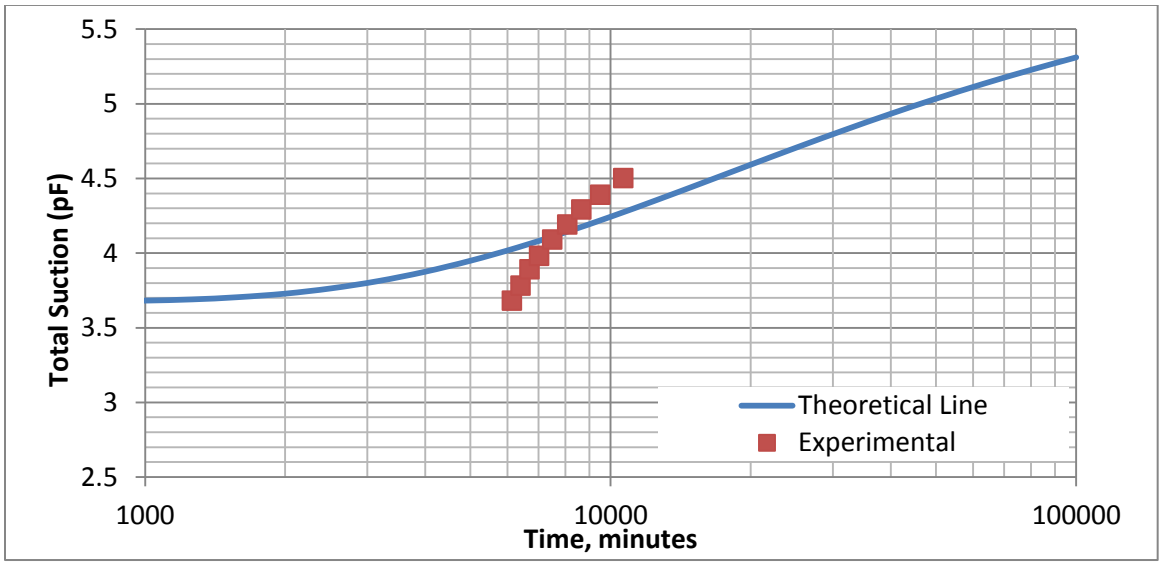

Figure H9. Variation of total suction with time for the soil of Ardmore site from boring 7, Soil segment 4AA2 at a depth of 0.95 to 2.0 feet

Table H10. Ardmore Site, Boring 7, Soil Segment 4DD3, Depth 6.85 to 7.50 Feet

Parameter	Value	Unit
Evaporation Coefficient, h_e	0.54	cm^{-1}
Atmospheric Suction, U_a	6.13	pF
Initial Suction, U_o	3.69	pF
Psychrometer Location, x	15	cm
Sample Length, L	17	cm

Drying Diffusion Coefficient, $\alpha_{dry} = 9.83 \times 10^{-6}$ cm^2/sec (5.9×10^{-4} cm^2/min)

Time	Suction
min	pF
3190	3.69
3310	3.76
3400	3.83
3520	3.90
3630	3.98
3800	4.05
3930	4.12
4050	4.19
4360	4.26
5070	4.34

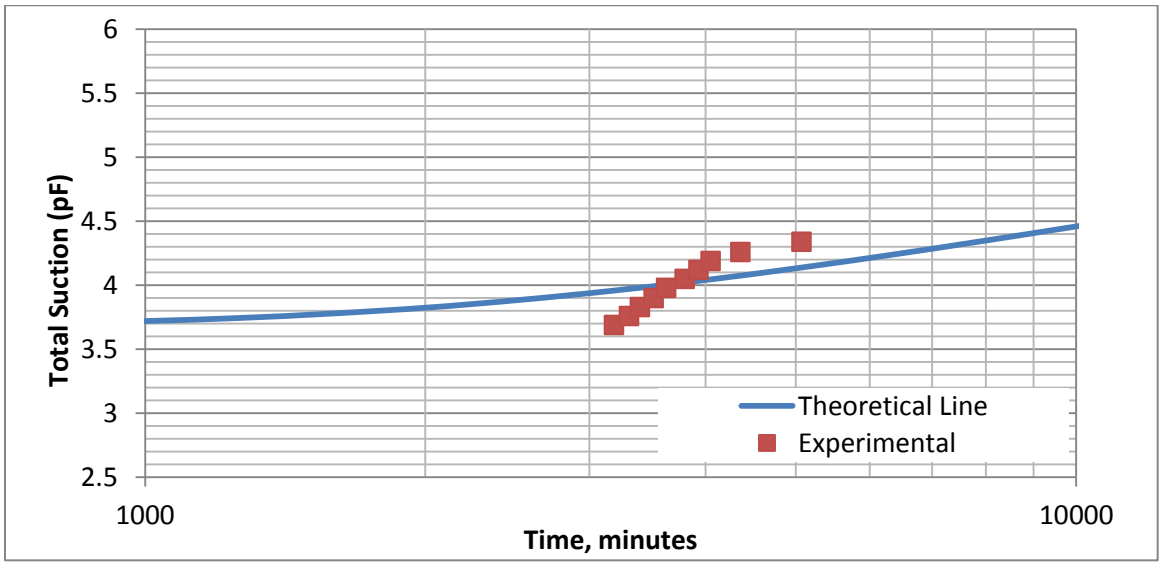

Figure H10. Variation of total suction with time for the soil of Ardmore site from boring 7, Soil segment 4DD3 at a depth of 6.85 to 7.50 feet

Table H11. Ardmore Site, Compacted Sample, Soil Segments 1A1, 1A2, 2A1, 2A2, Soil Type 1

Parameter	Value	Unit
Evaporation Coefficient, h_e	0.54	cm^{-1}
Atmospheric Suction, U_a	6.09	pF
Initial Suction, U_o	4.03	pF
Psychrometer Location, x	11.8	cm
Sample Length, L	16.8	cm

Drying Diffusion Coefficient, $\alpha_{dry} = 1.41 \times 10^{-5}$ cm^2/sec (8.5×10^{-4} cm^2/min)

Laboratory Suction Measurements

Time	Suction
min	pF
610	4.03
1610	4.10
2770	4.17
4000	4.25
5160	4.31
6600	4.38
8200	4.45
9700	4.52
11600	4.59
14690	4.66

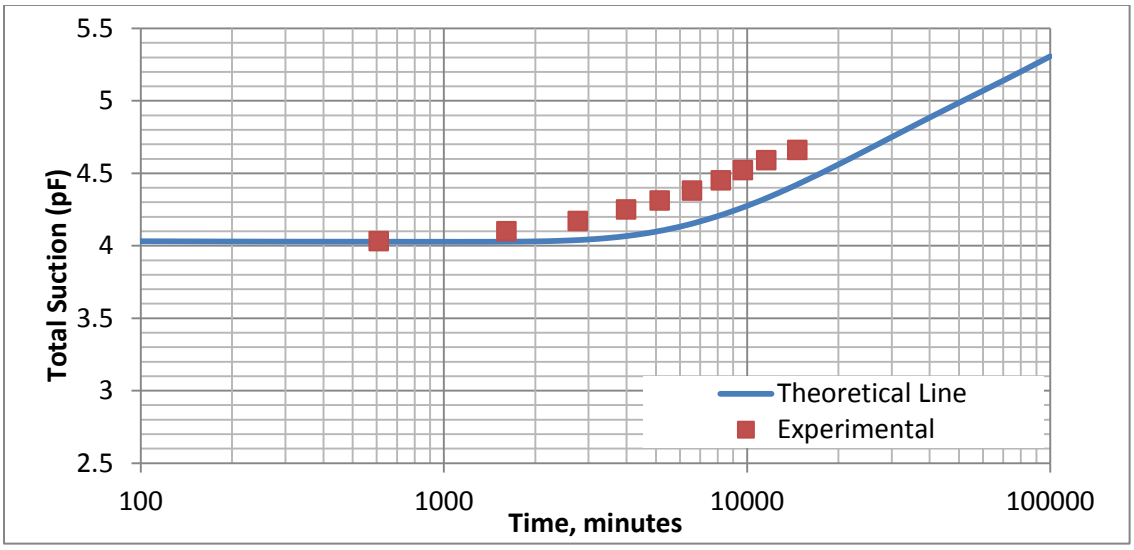

Figure H11. Variation of total suction with time for compacted samples of Ardmore Site soil from the segments 1A1, 1A2, 2A1, 2A2 of soil type 1

Table H12. Ardmore Site, Compacted Sample, Soil Segments 1B2, 2B1, 3B2, 1AA1, 1AA2, Soil Type 2

Parameter	Value	Unit
Evaporation Coefficient, h_e	0.54	cm^{-1}
Atmospheric Suction, U_a	6.09	pF
Initial Suction, U_o	3.69	pF
Psychrometer Location, x	13.5	cm
Sample Length, L	16.5	cm

Drying Diffusion Coefficient, $\alpha_{dry} = 1.22 \times 10^{-5}$ cm^2/sec (7.3×10^{-4} cm^2/min)

Laboratory Suction Measurements

Time	Suction
min	pF
2760	3.69
3270	3.79
3770	3.87
4390	3.95
5290	4.03
6490	4.12
8040	4.19
10090	4.28
12640	4.36
15890	4.44

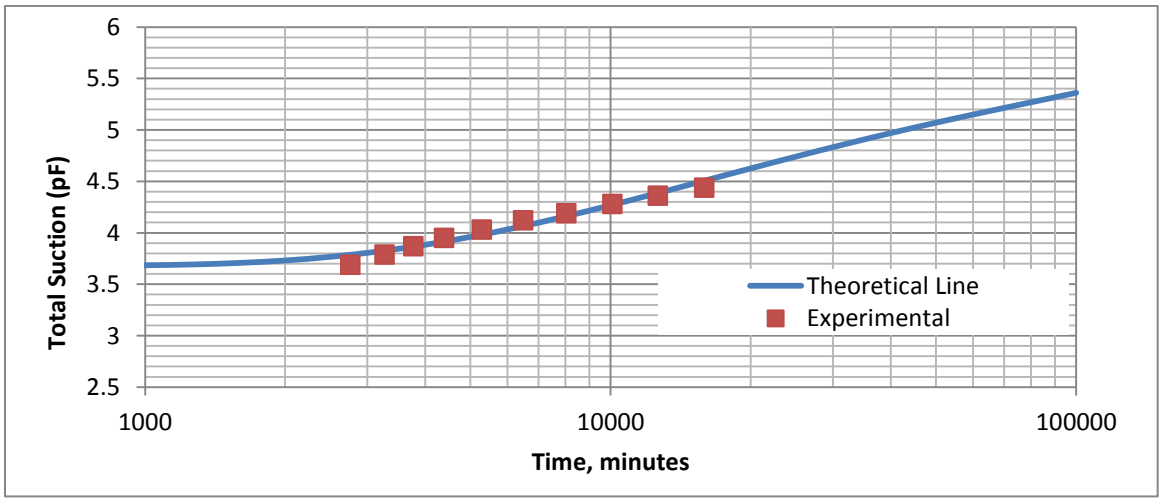

Figure H12. Variation of total suction with time for compacted samples of Ardmore Site soil from the segments 1B2, 2B1, 3B2, 1AA1, 1AA2 of soil type 2